Aus der

Universitätsklinik für Urologie Tübingen

Drug responses to Cisplatin, Venetoclax and S63845 on 3D organoids versus conventional 2D cell cultures of tumors of the urinary tract

Inaugural-Dissertation
zur Erlangung des Doktorgrades
der Medizin

der Medizinischen Fakultät
der Eberhard-Karls-Universität
zu Tübingen

vorgelegt von

Wei, Yi

2023

Dekan: Professor Dr. B. Pichler

1. Berichterstatter: Professor Dr. A. Stenzl
2. Berichterstatter: Professor Dr. M. Weiß

Tag der Disputation: 30.11.2022

Contents

List of figures

List of tables

List of abbreviations

UCs	Urothelial carcinomas
UTUCs	Upper tract urothelial carcinomas
BC	Bladder cancer
MIBC	Muscle-invasive bladder cancer
NMIBC	Non-muscle-invasive bladder cancer
RNU	Radical nephroureterectomy
2D	2-dimensional
3D	3-dimensional
CIS	Cisplatin
VTX	Venetoclax
S63	S63845
CK	Cytokeratin
FGFR3	Fibroblast growth factor receptor 3
BCO	Bladder cancer organoid
NUCs	Normal urothelial cells
UCC	Urothelial cancer cell
BME	Basement membrane extract
HCM	Hepatocyte culture media

1 Introduction

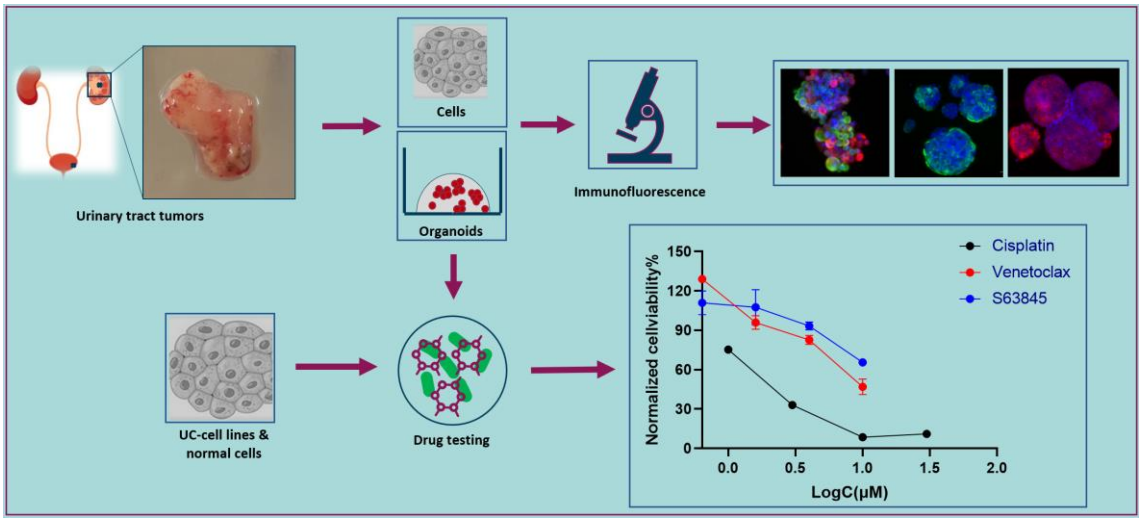

Figure 1: Flow-chart of the study

1.1 Upper tract urothelial carcinoma and bladder cancer

1.1.1 Epidemiology

Cancer is a major health problem around the world and is among the leading causes for death, coming in on second place e.g., in the United States. Prediction based on evidence computed that in 2021 around 608.570 people will die from cancer in America (Siegel RL et al. 2021). Urothelial carcinomas (UCs) is expected to be the 6th most common cancer in 2021 in developed countries (Siegel RL et al. 2021). According to anatomical location, they were divided into the upper (pyelocaliceal cavities and ureter) and the lower (bladder and urethra) urinary tract UCs. Upper tract urothelial carcinomas (UTUCs) are uncommon, and the incidence rate is only 5-10 % of all urothelial carcinomas (Siegel RL et al. 2021). A report predicted an annual incidence of almost around 2/100,000 residents in Western countries. Ureteral tumors occurred approximately in 50% of patients diagnosed with UTUC, while the other half presents with pyelocaliceal tumors. In addition, approximately one out of five cases is diagnosed with synchronous bladder

cancer (Cosentino M et al. 2013; Rouprêt M et al. 2020). However, bladder cancer (BC) is the most common malignancy in the urinary system with 90-95% of all urothelial carcinomas (Siegel RL et al. 2019). According to the recognized standard of TNM ("T" means the size of primary tumor or/and local extension of it; "N" means whether it involves the regional lymph nodes; "M" means distant metastasis) (Wittekind C et al. 2017) staging, only considering the depth of invasion (T stage) without "N" and "M", bladder cancer can be divided into muscle-invasive bladder cancer (MIBC) and non-muscle-invasive bladder cancer (NMIBC). Approximately 75-80% of bladder cancer cases are superficial, commonly referred to as non-muscle-invasive bladder cancer. Around 1/5 of NMIBC progress to invasive tumors (Grivas PD et al. 2011; Matulewicz RS et al. 2020). However, in spite of a lower incidence rate than NMIBC, MIBC usually means a very poor prognosis for the patient affected (Kamat AM et al. 2016; Prasad SM et al. 2011). In addition, close to 70 % of UTUCs were invasive at diagnosis, but this ratio in bladder cancer was 15-25 % (Margulis V et al. 2009).

1.1.2 Disease management

Regarding UCs management, appropriate surgeries are the golden standard for cancer therapy. But cancer treatment should be evaluated by clinical stage, tumor grade, and the relevant risk factors of the patient (Lerner SP et al. 2016; Resnick MJ et al. 2013; Seisen T et al. 2016; Rouprêt M et al. 2014). For localized nonmetastatic UTUCs, kidney-sparing surgery in low-risk tumors is the preferred strategy. Because radical nephroureterectomy (RNU) failed to result in better prognosis and mortality rate when compared to kidney-sparing surgery (Seisen T et al. 2016). In high-risk nonmetastatic and metastatic UTUCs, RNU is the standard therapy (Margulis V et al. 2009). But recent reports indicated that in metastatic UTUCs RNU could be performed in carefully selected cases with metastases only to one location (Moschini M et al. 2020; Nazzani S et al. 2019). In addition, endoscopic ablation (Cutress ML et al. 2012; Vemana G et al. 2016), ureteral resection

(Ou YC et al. 2018), should be considered with specific conditions. The management of BC by transurethral resection of the bladder (TURB) in combination with adjuvant treatment was recommend for all patients by EAU guidelines (Brausi M et al. 2002; https://uroweb.org/guideline/non-muscle-invasive-bladder-cancer/#7). In addition, many studies provided evidence that TURB in combination with neoadjuvant/adjuvant intravesical chemotherapy yielded lower disease recurrence and reduced mortality rates and the risk of progression (Matulewicz RS et al. 2020; Hosogoe S et al. 2018; Porten S et al. 2014) when compared to TURB alone.

1.1.3 Prognosis

Many distinct therapeutic strategies have been established and yielded beneficial effects. But the disease prognosis is still a limiting factor. Studies showed that the 5-year survival in stage pT2/pT3 tumors was less than 50% and only approximately 10% in pT4 of UTUC (Rouprêt M et al. 2013; Lughezzani G et al. 2012). We therefore need to develop a model to better recapitulate the disease and improve the prognosis, rather than only focus on conventional cell-lines or animal models. Recently, more and more research groups joined in using 3-dimensional organoid models to study and to improve this situation (Lancaster MA et al. 2019; Lee SH et al. 2018; Mullenders J et al. 2019; Pauli C et al. 2017).

1.2 Cell-lines

Cell-lines have been used as the models to investigate mechanisms of diseases for a long time, and for several reasons they are still key models in basic scientific research fields. Cell-lines are easily to maintain and can be employed for instance in experimental series to investigate responses of cells on molecular levels. Especially in cancer research, tumor cells in 2-dimensional (2D) culture systems partly recapitulate the ability of genomic aberrations in parent tumors (Goodspeed A et al. 2016). Such cells grant access to exploration of the molecular causes of the particular malignancy and may pave way for possible therapies. In general, such cell culture experiments are the fundament of modern cancer research to better understand its development and progression.

However, more and more studies reported the limitation of cell lines in research in the past few years. For instance, mammary cancer cell lines were not including the subtype of a specific form of cancer referred to as luminal A (Goodspeed A et al. 2016) and the relevant results from cell-lines were hard to repeat, so that the researchers faced difficulties to explain the results obtained and even made some erroneous conclusions. (Ben-David U et al. 2018; Freedman LP et al. 2015; Prinz F et al. 2011).

1.3 Organoids

In past several decades, more and more in vitro disease models have been explored. In this context, the 3-dimensional (3D) organoid culture system should be highlighted as a novel key technology in cancer research. In traditional experimental approaches, we usually focused our attention on cancer cells by themselves when exploring tumor growth. However, recent research showed clear facts, and we now understand the contributions of accompanying cells, such as endothelial and fibroblasts, for growth deregulation in a tumor in much more detail. These normal “bystander” cells play a key role for driving tumor cell proliferation (Hanahan D et al. 2010). This contribution of

“bystander cells” to the in vitro growth of tumor cells is one advantage of tumor organoids. Organoids therefore offer a way to explore in vitro the interplay of the tumor an its microenvironment under conditions much closer to the in vivo situation than standard 2D cell culture systems. In fact, the term or system “organoid” was coined for the first time more than seventy years ago. It was used to describe the features of tumors under the microscope at that time (Smith E et al. 1946). Recently another definition of “organoid” was introduced. It means an in vitro 3D structure containing cells and a matrix or scaffold as described in a recent publication (Sato T et al. 2009). The establishment of in vitro 3D structures was derived from stem cell research, including research employing embryonic and adult stem cells, induced pluripotent stem cells or embryonic progenitors, which can produce self-organized organoids in vitro and develop in their in vivo mimetics (Huch M et al. 2015).

Organoids derived from pluripotent stem cells were generated from tissue samples of brain, retinal, adenohypophysis, cerebellum, hippocampus, stomach, lung, thyroid, small intestine, liver, and others (Clevers H. 2016). These different types of stem cells were divided from pluripotent embryonic stems or from induced pluripotent stem cell lines (iPSCs) (Chen KG et al. 2014; Cherry AB et al. 2012). Organoids derived from adult stem cells were generated from small intestine, colon, stomach, liver, pancreas, prostate, mammary gland, fallopian tube, taste buds, lung, salivary gland, and esophagus. This suggested that organoids can not only be generated from pluripotent stem cells, but they also grow from adult stem cells when cultured in appropriate conditions (Clevers H. 2016).

One of the most important applications of human organoid cultures is to establish novel disease models to overcome the limitations of current research strategies. Compared to traditional 2D cell cultures, organoids grow in 3D structures, reflecting the micro-anatomy of the tissue of origin. Compared with most animal models, organoids provide human-derived tissues for experimental research. So far, organoid models were used to

mimic cystic fibrosis of the intestinal system (Dekkers JF et al. 2013), Leber congenital amaurosis (Parfitt DA et al. 2016), and infectious diseases (Ciancanelli MJ et al. 2015; Bartfeld S et al. 2015; McCracken KW et al. 2014). The personalized medicine developed by colon organoid-based cystic fibrosis testing (Dekkers JF et al. 2013) became the first personalized therapy test for a patient (Berkers G et al. 2019). In the meantime various types of cancer organoids were described (Sato T et al. 2011; Takebe T et al. 2013, Lancaster MA et al. 2013). In conclusion, human tissue- and tumor-derived organoids might be a new way to evaluate the effects of drugs and can supplement some of the animal tests required in pharmacological and toxicological research.

1.4 Immunostaining

Immunostaining was used to detect specific proteins by an antibody-based method in tissues and was adapted to research in histology, molecular and cell biology. Immunohistochemistry (IHC) pursues the investigation, in particular the biological features in tumor lesions. IHC markers were divided into four types: diagnostic, predictive, therapeutic and prognostic (Tsutsumi Y. 2021). The antibody referred to as AE1/AE3 is a pan antibody, which recognizes both high molecular weight and low molecular weight keratins, generally expressed in cancer cells of epithelial origin. The expression of high molecular weight keratins cytokeratin (CK) 5 and CK 8 and low molecular weight keratin CK 20, were used to characterize tissues of an epithelial origin. In bladder, cells expressing CK 5 are associated with a basal molecular subtype, and CK 8- and CK 20-positive cells are associated with a luminal molecular subtype. Furthermore research of cellular subtypes grants better understanding of cancer biology (Damrauer JS et al. 2014). Fibroblast growth factor receptor 3 (FGFR3) mutations are frequently found in bladder cancer. They were considered a key promoter of bladder cancer (Chae YK et al. 2017) and are being used as a the therapeutic target. The vimentin marker is an

intermediate filament protein which is expressed in mesenchyme cells rather than epithelial tissue.

The cell surface molecules CD47 and CD276 (B7-H3) are immune checkpoints antigens. They are ligands on tumor cells which combine with receptors on immune cells (Zhang Y et al. 2020). CD47 is broadly expressed in human cells. In contrast, CD276 protein is mainly expressed on tumor tissue rather than on normal tissue. Based on these features of immune checkpoints, novel therapeutic strategies using these targets for cancer therapy are currently being investigated of contribute to clinical feasibility studies to improve the cancer situation in the near future.

1.5 Cytotoxicity assay

A cytotoxicity assay is defined as test to determine the viability of cells in response to cytotoxic compounds. Cells may stop growing, undergo necrosis (= uncontrolled death), autophagy and apoptosis (= energy consuming controlled cell death) when exposed to cytotoxic substances. To evaluate potential pharmaceuticals or explore novel drug therapy strategies, cytotoxicity assays are frequently performed.

In our study, we compared two different reagents to measure the cell viability. Determining cell viability is based on the conversion of the water-soluble tetrazolium (WST) reagent in a colored dye through mitochondrial dehydrogenase. This enzyme is active only in viable cells. The dye generated diffuses in the medium of the well plate and the absorbance is recorded by a plate reader. The color generated was used to estimate the cell cytotoxicity. In a second series of experiments CellTiter Glo reagents were employed to measure metabolic or viability of cells. In this case, we measured ATP as indicator of

viability, and recorded ATP-dependent luminescence to evaluate the drug effects in comparison to the corresponding controls.

1.6 Drugs

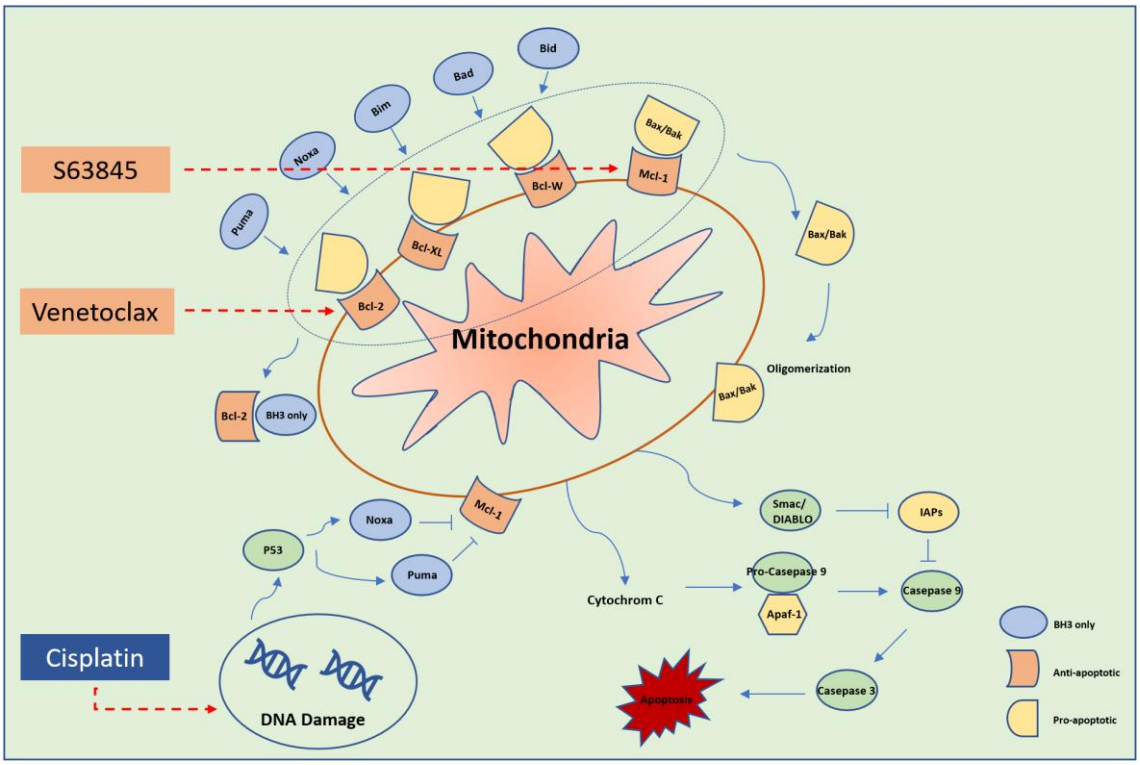

Figure 2: The mechanism of drug action. Cisplatin through DNA damage to cause cancer cells to apoptosis and was marked by blue color. Both Venetoclax and S63845 are belong to Bcl-2 families, but with different target to act the response. The intrinsic (mitochondrial) pathway is marked by orange color (adapted from https://www.medchemexpress.com/Targets/Bcl-2%20Family/bcl-2-family-signaling-pathway.html).

1.6.1 Cisplatin

Cisplatin is widely known and used as the first setting chemotherapy drug in different disorders such as lung-, ovarian-, breast- and bladder cancer (Dasari S et al. 2014). It acts through crosslinking the purine bases of DNA and thus inhibits the replication of DNA and obstructs DNA repair mechanism. This leads to DNA damage and induces cancer

cells to undergo apoptosis. In addition, members of the Bcl-2 family facilitate the release of cytochrome C in mitochondria to regulate DNA damage and then induce the apoptosis of cancer cells as well (Figure 2). Cisplatin has been unambiguously proved to be a therapeutic option for different types of cancers, such as sarcomas of bones, of soft tissue and muscles and carcinomas. Due to this clear pharmacological mechanism and effects, cisplatin is an excellent drug and was selected to test drug responses in the novel 3D organoid model. It was uses as standard reference to evaluate the effects of other drugs.

1.6.2 BH3-mimetics: Venetoclax and S63845

A hallmark in most and maybe all different types of cancer is their acquired resistance towards apoptosis (Hanahan D et al. 2011; Holohan C et al. 2013). The apoptotic program almost exists in all types of cells in a latent form. The hypothesis that apoptosis might be a barrier to intervene tumor growth was proposed some 50 years ago (Kerr JF et al. 1972). With the development of cancer research, anti-apoptotic mechanisms of cancer cells have been proved to be promising therapeutic strategy. Among other chemicals, “BH3-mimetics” represent one of the important and promising compounds in this context (Villalobos-Ortiz M et al. 2020). BH3 is the only pro-apoptotic protein belonging to the Bcl-2 family. Through interactions with other components at the outer membrane of mitochondria BH3 will determine whether Bax/Bak will change their structure, oligomerize and then cause apoptosis (Figure 2). Inhibition of the anti-apoptotic proteins of the Bcl-2 families has been proved to be inefficient, because the small molecules can’t be blocked completely by components applied so far (Villalobos-Ortiz M et al. 2020). Therefore, more research is needed to develop this field and to evaluate the effects of novel BH3-mimetics.

Venetoclax and S63845 have already been proved true BH3-memitics (Villalobos-Ortiz M et al. 2020). The drug venetoclax is used to treat blood cancer and yielded clear positive

effects in clinical trials. But to the best of my knowledge, it was never used to therapy urological cancer in the past. The same situation is noted for S63845. In particularly, this compound is a purely experimental chemical. So, patient-derived organoids are an interesting attempt to evaluate the impact of these compounds in urological cancers.

1.7 Aim of the study

Patient-derived organoids have found an ever-increasing interest in basic research as well as in pre-clinical and clinical work. More and more valuable applications were reported during the past decades. But research progress is still in a kind of early stage, particularly in urology, as protocols to generate stable bona fide organoids are not standardized to a satisfactory level. Therefore, it needs more investigations to develop this field.

The purpose of this thesis was to generate a method to establish patient-derived organoids from urothelial carcinomas, including upper tract urothelial and bladder carcinoma. The aim of this work was to prove whether they are bona fide UC organoids and to characterize some biological features of them by analysis of marker gene expression. Employing the organoid lines generated, cytotoxicity assays were used to perform cytotoxicity analyses with cisplatin, venetoclax and S63845, respectively. In addition, autologous conventional 2D cells were used to test the drug response in adherent cultures as well. In conclusion, this thesis was designed to explore whether urothelial carcinoma cells in 3D organoid systems responded to the drugs, and if these responses reveal differences between 3D organoids and conventional 2D cultures.

2 Materials & Methods

2.1 Equipment

Table 1: Equipment

Equipment	Manufacturer
Cell Incubator	Binder
Biological Safety Cabinets MSC 1.5	Thermo
Platform Scale 770 1mg	KERN
Centrifuge 5424	Eppendorf
64R Centrifuge	Allegra™
Centrifuge	Lab Technology
FVL-2400N Euro Plug	Biosan Sia
LSM 510 Laser Microscope	Zeiss
Axiovert 200M Microscope	Zeiss
Axiovert A1 Microscope	Carl Zeiss
Lightcycler 480-II	Roche
Electrical pipetting device	Eppendorf
Pipette 0.5 – 10µl. 10 – 100µl. 20 – 200µl. 100 – 1000µl	Eppendorf
Pipetboy	Hirschmann
Stirrer Reax Top	Heidolph
Water Bath WBT 22	MedingLab
Refrigerator -80°C	Sanyo and Skadi
Refrigerator 4°C and -20°C	Liebherr
GloMax GM3500	Promega

Nano Photometer NP80	Implen
Thermal Cycler UNO-2	Biometra

2.2 Consumables

Table 2: Consumables

Consumables	**Manufacturer**
Pipette 2 ml, 5 ml, 10 ml, 25 ml, 50ml	Corning
Pipette tips	Eppendorf
epT.I.P.S. Standard	Eppendorf
Petri dish	Greiner bio-one
Safe-lock Tubes 1.0 ml, 1.5 ml, 2.0 ml	Eppendorf
Tubes 15 ml, 50 ml	Greiner Bio-one
Cryovial 2.0 ml	Thermo Scientific
24-well, 48-well, 96-well cell culture plate	Corning
6 well culture plate	Corning
Opaque 96-well plate	Costar
Decosept Sensitive	Dr. Schumacher
Medical Examination Gloves	Abena
Disposable Scalpel 20x	Feather
Flask 25 cm^2, 75 cm^2	Falcon
Filter Tips 200 µl	Biosphere Plus69
Disposable Counting Chambers (DHC-N01)	NanoEntek
Premium Tips 1 ml (free of DNase and RNase)	Biozym

Parafilm	Pechiney
PCR Tube Strips 0.2 ml	Eppendorf
X-well Tissue Culture Chambers	Sarstedt AG
C-Chip DHC-N01	NanoEnTek
Filter 70-µm, 100-µm	Greiner bio-one

2.3 Chemicals, enzymes, reagents

Table 3: Chemicals, enzymes and reagents

Material	**Supplier**
Advanced DMEM/F12(1X)	Gibco
DPBS (Dulbecco's Phosphate-buffered saline)	Gibco
Collagenase Typ II (3000U/ml)	STEMCELL Tech
Trypanblue	Sigma-Aldrich Chemie
Hepatocyte Culture Media	Corning
epidermal growth factor (EGF)	Corning
Glutamax 100X	Invitrogen
Primocin	Invitrogen
Cultrex Basement Membrane Extract, Type 2	Bio-Techne
Y-27632 dihydrochloride	MedChemExpress
FBS (Fetal bovine serum)	Sigma-Aldrich Chemie
Charcoal dextran-coated, C6241	Sigma-Aldrich Chemie
FGF 7 (Fibroblast growth factor)	PeproTech
FGF 10	PeproTech
FGF 2	PeproTech

B27 supplement	Gibco
A 83-01	Tocris
N-Acetylcystein	Sigma-Aldrich Chemie
Nicotinamide	Sigma-Aldrich Chemie
Dispase II(D4633)	Sigma
TrypLE(1X)	Gibco
DMSO (Dimethyl-sufoxid)	AppliChem
RPMI Medium 1640	Gibco
Lightcycler 480 SYBR Green I	Roche
Rnase Fibrous Tissue Mini Kit	Qiagen
Dnase Blood and Tissue kit	Qiagen
Advantage RT-for-PCR kit	Takara
WST-1 reagent	Roche
CellTiter-Glo® 3D reagent	Promega
CellTiter-Glo® 2.0 reagent	Promega
MEM Earle's-FG 0325	Bio-sell
FBS	Sigma
MEM Non-Essential Amino Acids (100X)	Gibco
HEPES(1X)	Gibco
DAPI	Jackson ImmunoResearch
Goat-anti-mouse IgG Cy3	Jackson ImmunoResearch
Goat-anti-rabbit IgG Alexa FI.488	Jackson ImmunoResearch
Mouse-anti-cytokeratin AE1/AE3 Antibody	Millipore, MAB3412
Rabbit-anti-cytokeratin 5	BioLegend, 905504
Cytokeratin 8 Monoclonal Antibody	Invitrogen, MA5-14088
Cytokeratin 20	DAKO, M7019

Mouse Anti-Vimentin	Becton Dickinson, 550513
CD 47 Monoclonal Antibody(B6H12)	Invitrogen, 14-0479-82
Anti-CD276 antibody	Abcam, ab226256

2.4 Buffers and Solutions

Table 4: Buffers and solutions

Buffer	**Ingredients**
Transport medium	500 ml Advanced DMEM/F12(1X) 1 ml (50mg/ml) Primocin
HCM medium	500 ml Hepatocyte Culture Media 5 µg Epidermal growth factor (EGF) 5 ml (100X) Glutamax 1 ml (50mg/ml) Primocin
MEM medium	500 ml MEM Earle's 10% FBS 1% NEAA 0.2% Primocin
Organoid culture medium (OCM)-1 (HCM+5% csFBS)	95% HCM 5% csFBS
Organoid culture medium – 2	95% HCM 5% csFBS 0.1% Y-27632
Organoid culture medium – 3	12. 5 µl FGF 7 12. 5 µl FGF 2 50 µl FGF 10 50 µl A83-01

	125 µl N-Acetylcystein 500 µl Nicotinamide 1 ml B27(50X) 48. 25 ml ADMEM/F12 medium
Freeze medium	50% RPMI Medium 1640 30% csFBS 20% DMSO
Splitting medium	50 ml Advanced DMEM/F12 500 µl HEPES 500 µl L-Glutamine
Blocking solution	5% BSA (2.5 g in 50 ml PBS, 10 min, 37 °C, 5% CO2 → filtration 0.45µm) 0.2% Triton-X-100(100 µl) 0.1% Tween 20(50 µl with cup tip)
Primer mix	NTC water 400 µl Forward primer 50 µl Reverse primer 50 µl
Master mix for qRT-PCR	SYBRgreen 10 µl NTC water 6 µl Primer mix 2 µl
Master mix for reverse RNA to cDNA	4 µl 5x buffer 0.5 µl Rnase inhibitor 1 µl dNTP mix 1 µl reverse transcriptase

2.5 Cell lines

Table 5: Cell-lines

Cell line	Reference
RT 4	ATCC, HTB-2
HT 1197	ATCC, CRL-1473

2.6 Tissue samples

Table 6: Information of selected tissues samples

Line and tissue origin	Sex	Age	Tumor stage	Pathologic classification	Smoking	Prior therapy before surgery	Surgery type	Primary/ Recurrence
BCO#41* BC Tumor	M	77	Ta	Low-grade urothelial carcinoma	Yes	No	TURB	Primary
BCO#44* Lymph nodes	F	81	T3a	squamous cell carcinoma	Passive smoking	No	Cystectomy	Primary
BCO#56* UTUC Tumor	F	74	T3	High-grade urothelial carcinoma	No	No	Nephro-ureterectomy	Primary
BCO# 107 BC Tumor	M	70	T1	High-grade urothelial carcinoma	Yes	No	TURB	Primary
BCO# 136 BC Tumor	M	57	T2a	High-grade urothelial carcinoma	Yes	No	TURB	Primary
BCO# 140 BC Tumor	M	62	T1	Small-cell carcinoma	Yes	No	TURB	Primary
BCO# 147 UTUC Tumor	M	59	T4	High-grade urothelial carcinoma	Yes	No	Nephro-ureterectomy	Recurrence

*These BCOs were prepared together with Leander Schwaibold and will therefore be also part of his medical thesis. All other BCOs were prepared and explored by myself.

2.7 Primary organoid cultures

Patient derived tissues were obtained from the surgery samples and immediately submerged in centrifugation tubes filled with transport solution and shipped on wet ice to the laboratory. Then tissue was placed in a petri dish to determine the wet weight, covered with transport solution, and dissociated by aid of a scalpel in tiny pieces. The samples were sedimented by centrifugation (480g, 10 minutes, ambient temperature), the supernatant was removed, and the pieces were resuspended in HCM complemented with Collagenase Typ II (2 × 30minutes, 3000U/ml, 37°C, 5% CO_2). To remove debris, the digested tissue was filtered (70-µm or/and 100-µm), and the cells were sedimented by centrifugation (150g, 5 minutes, ambient temperature). The yield of cells was determined by aid of a hematocytometer using trypan blue dye exclusion and computed (see 2.9.). Aliquots of Matrigel were prepared on wet ice. 20,000 cells suspended in 10 µl medium were mixed with 30µl Matrigel on ice and 40µl mixed solutions of cells with Basement Membrane Extract (BME) was planted into one well of a 24-well plate. The plate was flipped headlong 180° to generate a hanging drop and incubated at 37°C, 5% CO_2 for 15 minutes in humidified atmosphere to harden the hydrogel. After that, the plate turned 180° again, and 500 µl organoid culture medium was added to each well. During the first 7 days, Rock inhibitor Y-27632 (10 µM) was included in the organoid culture medium to avoid cellular apoptosis (This method is improved based on "Mullenders J et al. 2019").

2.8 Primary cell-culture in 2D

2.8.1 Tissue origin cell-culture in 2D

For some experiments, normal 2 dimensional (2D) adherent cell cultures were prepared from surgical specimen of human urothelial cancer tissue samples. In brief, the tissue was dissociated by scalpel, sedimented, degraded by collagenase, filtered, and the yield of cells was enumerated as described above (see 2.7). The cells were resuspended in MEM medium and cultured in 6-well plates with 3 ml MEM medium per well. For tiny tissue processing, dissection of the samples was omitted, samples were degraded by proteolysis only, and directly seeded in culture medium.

2.8.2 Organoids origin cell-culture in 2D

In some cases, 3D organoids were established but the corresponding normal 2D cultures were missing. As surrogate for normal 2D cultures, organoids were harvested to isolate the cells using the organoid passaging methods (2.10). But the last step, after digestion by dispase II and TrypLE, cells were washed, and cultured in flask in MEM medium.

2.9 Counting cells/organoids

The establishment of organoid and cytotoxicity assay should be performed in the suitable concentrations of organoids/cells. To obtain the preparation concentrations of organoids/cells, counting organoids/cells according to the formula:

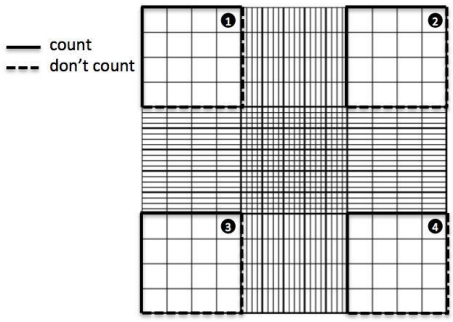

(Cite from: www.protocols.io/view/counting-cells-with-hemocytometer-nxsdfne.html)

$$C_{(concentration)} = \frac{①+②+③+④}{4} \times 2 \times 10^4\ cells/ml$$

Totally 40 µl mixed solution (20 µl organoids/cells suspension with 20 µl trypan blue) was added to counting chambers. For the special counting of organoids of cytotoxicity assay, a single cell or cell cluster was counted as the number 1 to calculate the numbers of organoid.

2.10 Splitting organoids

Organoids should be passaged when grown dense, or when the 3D structure start to disintegrate. First, the suitable splitting ratio (in most cases ≤ 1:5) should be determined under the microscope. For cell harvesting, the organoid culture medium was aspirated and replaced by HCM without csFBS complemented with dispase and incubated (1 hour at 37°C, 5% CO_2, humidified atmosphere). Next, the organoid suspension was centrifuged at 150g for 5 minutes. The supernatant was aspirated, the pellet was resuspended in TrypLE, and incubated for 5 minutes at room temperature. Using the pipette, organoids were dissociated to individual cells. To stop the proteolysis, the centrifugation tube was filled up with organoid culture medium and cells were sedimented by centrifuge at 150g for 5 minutes. Next, the supernatant was removed, and the cells were resuspended in 40 µl mixed solutions of organoids in medium complemented by Basement Membrane Extract. The mixture was planted into the middle of the well and the plate was tilted over headlong (180°) and incubated at 37°C, 5% CO_2 for 15 minutes. After that, the plate 180°

was turned around again, and 500 µl organoid culture medium per well per well were added to the construct in a 24-well plate. (This method is improved based on "Mullenders J et al. 2019").

2.11 Freezing organoids

To store organoids and secure back-up samples, the BME matrix was digested by dispase II for 1 hour at 37°C, 5% CO_2. After incubation, the suspension containing organoids was centrifuged at 150g for 5 minutes. Next, the organoids were resuspended in 1 ml organoid culture medium and mixed gently with 1 ml ice-cold freezing medium. Then the organoids were transferred into cryopreservation tubes, slowly cooled to – 20 °C, and stored for no more than 4 weeks at -80 °C until further use. For long-term storage, the organoids were transferred in a liquid nitrogen tank.

2.12 Thawing organoids

Cryopreservation tubes were retrieved from the -80°C deep freezer or from the liquid nitrogen tank were transported on ice to the 37 °C water bath as quickly as possible. The organoids were thawed in less than 1 minute. Then organoids were resuspended in 10 ml prepared warm cultured medium and were sedimented by centrifugation at 150 g for 10 minutes. The supernatant was removed. The ice-cold organoid suspension mixed with BME stock solution (40 µl total) was planted into the middle of the well, the plate was tilted over (180°) and incubated at 37°C, 5% CO_2 for 15 minutes to generate hanging drops. After that, the plate was turned around again. Then 500 µl organoid culture medium was added into per well in 24-well plate.

2.13 Fixation of organoids

After selecting 4-5 wells of well grown organoids for fixation per chamber slide, the organoid culture medium was replaced by HCM (without csFBS) with dispase II and incubated for 1 hour at 37°C, 5% CO_2. Next, the organoid suspension was centrifuged at 150g for 5 minutes. The supernatant was removed, and the sediment was resuspended in TrypLE and incubated for 5 minutes at room temperature. By pipetting up and down the organoids were resuspended to individual cells. Then, the tube was filled up with organoid culture medium and centrifuged at 150g for 5 minutes. Carefully remove the supernatant down to 20 – 30 µl. Next, 1160 µl cold splitting medium and 40 µl BME with organoids resuspension were added for 8 chambers (150 µl per chamber). After incubation for 2 hours at 37°C, 5% CO_2, 250 µl 4% PFA per chamber was added and incubated for 30 minutes at the room temperature under the fume cupboard. Then 250 µl PFA was removed and washed with 250 µl PBS per chamber for 3 times × 5 minutes at room temperature. 250 µl blocking solution were added per chamber and incubated for 1 hour at 37°C, 5% CO2. Moreover, samples were washed with 250 µl PBS-T per chamber for 5 min at room temperature and then stored at 4°C until staining (≤ 1 week).

2.14 Immunofluorescence staining: chamber slides

Immunofluorescence staining was used to characterise organoids. The PBS was removed from the fixed organoids. Antibodies were diluted to concentrations predetermined in preliminary tests in 1% BSA/PBS-T. Then 100 µl antibody solution per chamber was added and incubated for 1 hour at 37°C, 5% CO2 in a humid chamber. Next, the antibody solution was removed and the samples were washed three times for 3min with 250µl PBS per chamber. The fluorescence-labelled secondary antibody was diluted in 1% BSA/PBS-T (1:1500), DAPI (1:1000) was added, and the samples were incubated at room temperature for 1 hour in humid chamber. The antibody/DAPI solution was poured off

and the samples were washed with 250µl PBS per chamber three times for 3 minutes. At the end, the samples were covered with Dako mounting medium and cover glasses.

2.15 RNA Extraction using Rneasy Kit from Quiagen

To quantify the expression of immune checkpoint proteins organoid cultures, RNA was extracted, revers transcribed to generate cDNA, and quantitative real-time polymerase chain reaction (qPCR) was used to enumerate the transcripts. Expression of GAPDH and PPIAγ were investigated to normalize the expression of the target gene using the differences of the crossing points of the cDNA amplification (Δcp) (Rasmussen R et al. 1998).

The organoid was digested by dispase II and TrypLE, respectively as described above (see 2.10.). The cells were transferred in a 50 mL centrifugation tube, washed by medium and sedimented by centrifugation (1,500rpm, 7 minutes). RNA was extracted as requested by the supplier of the kit. The cells were washed by 10ml cold PBS by centrifugation and resuspended in 350µl RLT buffer containing β-mercaptoethanol to isolate RNA. This raw extract was stored at -70 °C for 2 hours. After that, the extract was thawed on wet ice and 350µl of the 70 % ethanol was added. The extract was homogenized by aid of needle (G20) and syringe and transferred to a Qiagen RNA extraction column. Then the column was centrifuged at 10,000 rpm for 15 seconds. The flow-through fraction was discarded. 350 µl RW1 (RNA washing buffer) were added to the column and centrifuged again at 10,000 rpm for 15 seconds. The flow-through fraction was discarded. Next, 80 µl of DNase were added on the column and incubated for 15 minutes at room temperature to reduce DNA contaminations. The DNase was washed off by 350 µl RW1 buffer and centrifugation at 10,000 rpm for 15 seconds. The flow-through fraction was discarded. 500 µl of RPE buffer was added and spun at 10,000 rpm for 15 seconds. The flow-through was discarded again. 500 µl of RPE buffer were added and the column was centrifuged

at 10,000 rpm for 2 minutes. By centrifugation at 10,000 rpm for 15 seconds the columns were dried and the flow-through was discarded. Then, the column was placed in a new tube and 40µl of RNase-free water were added and incubated for 1 minute. The purified RNA was collected in the new tube by centrifugation at 10,000 rpm for 1 minute. The flow-through containing RNA was stored at – 70 °C until reverse transcription in cDNA.

2.16 Reverse Transcription of RNA into cDNA

The reagents for reverse transcription were fetched from – 20 °C freezer, thawed on ice, vortexed, shortly centrifuged, and then put on the ice. The RNA sample was fetched from the – 70 °C deep freezer, thawed and put on the ice as well. 1µl RNA extract was used to measure its concentration by UV-spectrophotometry (C_{RNA}, Nano Photometer NP80, Implen, 260nm). The volume of RNA (V_{RNA}) equivalent to 1µg was determined by the formula:

$$V_{RNA} = \frac{1000 \text{ ng}}{C_{RNA} ng/\mu l}.$$

1µg of total RNA was added to a microtube and filled up to 12.5µl with DEPC water. The RNA solution was mixed, centrifuged, and 1µl of oligo dT primer solution was added. Next, the sample was put in a PCR block, and heated at 70°C for 2 minutes to melt RNA double strands. The solution was quenched on wet ice and 6.5µl of cDNA synthesis master-mix (Table 7) were added. The cDNA synthesis was performed as requested by the supplier (Advantage RT-for-PCR kit TakaraBio, Saint-Germain-en-Laye, France). The sample then was placed in the PCR block and incubated in the device at 42 °C for 1 hour. At the end, 80 µl of DEPC water were added, the sample was heated for 60 seconds at 90°C to remove the enzymes from the cDNA-RNA heteroduplexes and to denature these proteins. Then the sample was stored at – 20 °C.

Table 7: The Master-mix for reverse transcription of RNA to cDNA

Reagent	Volume
5 x buffer	4µl
RNase inhibitor	0.5µl
dNTP-Mix	1µl
Reverse transcriptase	1µl

2.17 Quantification of CD276 and CD47 mRNA transcription with qRT-PCR

The qRT-PCR was performed by a LightCycler 480 System. The reagents of Sybr green, Primer-mix, non-template water and cDNA were mixed in a well of a 96-well PCR plate, collected in the well tips by centrifugation, and put it on the ice until using. The peptidylprolyl isomerase A (PPIA) and glyceraldehyde 3-phosphate dehydrogenase (GAPDH) were used as the reference genes, often referred to as "housekeeping gene" or "internal standard" to normalize the expression of target genes investigated in each extract, cDNA batch, and amplification reaction. In a 96-well plate, 2µl of smooth muscle cells (SMC) cDNA was first pipetted into the well which was used as the positive control. 2µl of non-template water as the negative controls were placed for each sample after that. Subsequently, 18 µl of the master-mix were dispensed in each sample well. Then the 96-well plate was covered with a transparent film and centrifuged at 1,000rpm for 1 minute. The PCR amplification was performed by a LightCycler 48 (Roche) as described in (Table 8).

Table 8: Features of target marker gene by qRT-PCR

Program	Temperature	Time	Cycles
Denaturation	95°C	5s	1
Amplification	95°C - 60°C- 72°C	10s – 20s – 30s	39

Melting Curve	95°C - 60°C - 97°C	5s – 30s – cont.	1
Cooling	40°C	30s	1

2.18 Cytotoxicity Assay of 2D cells

2.18.1 Testing cells preparation

Normal urothelial cells (NUCs) were prepared from ureter samples of patients undergoing kidney surgery at UKT (ethics committee approval #804-2020-B02) and expanded as described (Aicher WK et al. 2021). Bladder tumor cell-lines RT4 and HT1197 (ATCC Manassas, VA, US) were expanded as requested from the supplier. At the beginning, each of NUCs, RT4 and HT1197 were use at an inoculation dose of 5,000 and 10,000 cells/96-well plate. However, as cytotoxicity testing was performed for up to 4 days, the seeding density of the cells was titrated to obtain sufficient numbers of cells for 24 hours incubation times, yet to avoid cell confluence after 72 hours or 96 hours of incubation. Confluence was expected to bias the drug test results.

Patient-derived urothelial cancer cell (UCC) cultures were the other source for 2D cells (ethics committee approval # 804-2020-B02). The tissues from the surgery were divided into two parts. One part was utilized for production of organoids, the remaining part was used for preparation of UCCs in 2D cultures. The UCCs were characterized and expanded as described (Aicher WK et al. 2021). In some cases, the amount of tissue obtained for cell isolation was not sufficient to generate organoids and 2D UCC cultures. In these cases, organoids were produced in the first place. Upon splitting an aliquot of cells was set aside and transferred to 2D cell culture. This was a feasible way to perform this drug testing in 3D vs. 2D cultures.

The cells were expanded to achieve enough cells for the drug tests. To prepare the cells for the assays, the cell culture medium was aspirated, and the cells were washed twice by PBS. The cells were detached enzymatically by 1.5ml TrypLE (75 cm^2 flask) for 5minutes

at 37°C, 5% CO2. After shaking the flask, 4.5ml of cell culture medium were added to stop digestion. Cells were sedimented by centrifugation at 480g for 5 minutes. and resuspended in 1 – 10mL medium to determine yield and viability of cells (see 3.10.). Then obtain the aim concentration of cells and planted 100 µl cell suspension to each well.

2.18.2 Drug preparation

Cisplatin (CIS, Sigma-Aldrich, Germany) was chosen as the standard reference of the drug testing. The original testing concentration were 66µM, 33µM, 25µM, 12.5µM, 6.25µM, 3.125µM, 1.5625µM, respectively. Venetoclax (VTX, Selleck Chemicals, Huston, TX, USA,) is a BCL-2 inhibitor. S63845 (S63; Selleck Chemicals, Huston, TX, USA) is an MCL-1 inhibitor, a member of BCL-2 family. Venetoclax was used as a chemotherapy drug to blood cancer, but never reported in preclinical studies of urothelial cancer. In contrast, S63845 is at present an experimental drug only. However, S63845 may become a bladder cancer drug in the future. Therefore, we compared it to CIS and to VTX before clinical feasibility studies could be initiated. In the first series of experiments, concentrations of VTX and S63845 were 25µM, 10µM, 4µM, 1.6µM, 0.64µM, 0.256µM, 0.1024µM, respectively. Untreated cells or solvent only samples (DMSO) served as controls.

For the cytotoxic assays, the drugs were diluted to the final concentrations needed by cell culture medium. To this end, 100µl drug solution in medium was prepared for each testing well (96-well plate). For the assay, the cell culture medium was replaced by drug solution diluted in medium in each well and incubated in a cell culture incubator at 37 °C, 5 % CO2 for 24 hours, 48 hours, 72 hours and 96 hours, respectively.

2.18.3 WST assay

According to the introduction of use from the company, 100µl of WST solution was directly added to each testing wells. The reagents were mixed for 30 seconds and incubated for 2 hours at 37 °C, 5 % CO2. Then record the absorbance values were measured at 440nm by a plate reader (GloMax).

2.18.4 CellTiter-Glo 2.0 assay

Due to the experimental conditions of CellTiter-Glo 2.0 reagent, opaque 96-well plates must be used. Prior to the assay, plates were transferred to the sterile workbench to equilibrate it and its contents at room temperature for approximately 30 minutes. Subsequently, 100µl of CellTiter-Glo 2.0 reagent were added in each well (Figure 3, 4) and incubated for another 10 minutes at room temperature. At the end, luminescence was measured by the GloMax plate reader using an integration time of 0.3 seconds per well.

	1	2	3	4	5	6	7	8	9	10	11	12
A												
B		Blank	Blank	Blank	Blank	Blank	Untreated + Cells	Untreated + Cells	Untreated + Cells	Untreated + Cells	Untreated + Cells	
C		CIS, VTX/S63 + Cells	CIS, VTX/S63 + Cells	CIS, VTX/S63 + Cells	CIS, VTX/S63 + Cells	CIS, VTX/S63 + Cells	DMSO + Cells	DMSO + Cells	DMSO + Cells	DMSO + Cells	DMSO + Cells	
D		CIS, VTX/S63 + Cells	CIS, VTX/S63 + Cells	CIS, VTX/S63 + Cells	CIS, VTX/S63 + Cells	CIS, VTX/S63 + Cells	DMSO + Cells	DMSO + Cells	DMSO + Cells	DMSO + Cells	DMSO + Cells	
E		CIS, VTX/S63 + Cells	CIS, VTX/S63 + Cells	CIS, VTX/S63 + Cells	CIS, VTX/S63 + Cells	CIS, VTX/S63 + Cells	DMSO + Cells	DMSO + Cells	DMSO + Cells	DMSO + Cells	DMSO + Cells	
F		CIS, VTX/S63 + Cells	CIS, VTX/S63 + Cells	CIS, VTX/S63 + Cells	CIS, VTX/S63 + Cells	CIS, VTX/S63 + Cells	DMSO + Cells	DMSO + Cells	DMSO + Cells	DMSO + Cells	DMSO + Cells	
G												
H												

Figure 3: The template of cytotoxicity assay in CellTiter Glo 2.0 reagent.

2.19 Cytotoxicity Assay of 3D organoids

2.19.1 Testing organoids preparation

To discriminate random cell clusters from *bona fide* organoids, patient- derived organoids were utilized only after passaging the cells for 5 splittings and seeding cells in fresh domes. The cytotoxicity assay was performed with organoids in their 5^{th} passage, or higher.

Due to the limitations of the detection technique and according to the guidelines of the reagent, the diameter of organoids to be tested by CellTiter-Glo 3D-chemistry in the corresponding plate reader must be limited to less than 300µm. Therefore, the mean size each of the organoids was checked under the microscope before testing the cytotoxicity. After that, the BME was digested by dispase II for 1 hour at 37 °C, 5% CO_2. The dispersed samples were sedimented by centrifugation at 150g for 5 minutes and resuspended in organoid culture medium. The organoids were counted and diluted to achieve well form for the drug testing containing 1,000 – 2,000 organoids per milliliter. Lastly, 100µl of organoid solution, including 3 - 5µl BME, were seeded in each well. Then incubated for 24 hours, 48 hours and 72 hours.

2.19.2 Drug preparation

Organoids grow in a matrix in 3D constructs. Therefore, culture medium or drugs cannot be exchanged by aspiration and replacement while doing drug testing. Therefore, the drug testing protocols were different between adherent cells and organoids. For drug tests of organoids, 1µl of drug a corresponding stock solution was added per well to obtain the concentration required. Then the well plates were incubated at 37°C, 5% CO_2 for the timespan needed.

2.19.3 CellTiter-Glo 3D assay

According to the CellTiter-Glo 3D reagent s synopsis, the 96-well plate and its contents was incubated at room temperature (20 – 25 °C) for approximately 30 minutes to equilibrate. Next, 100 µl CellTiter-Glo 3D assay reagent was added in each well (Figure 4) and incubated for 25 minutes at room temperature. Then luminescence was recorded by a plate reader (GloMax) using an integration time of 0.3seconds per well.

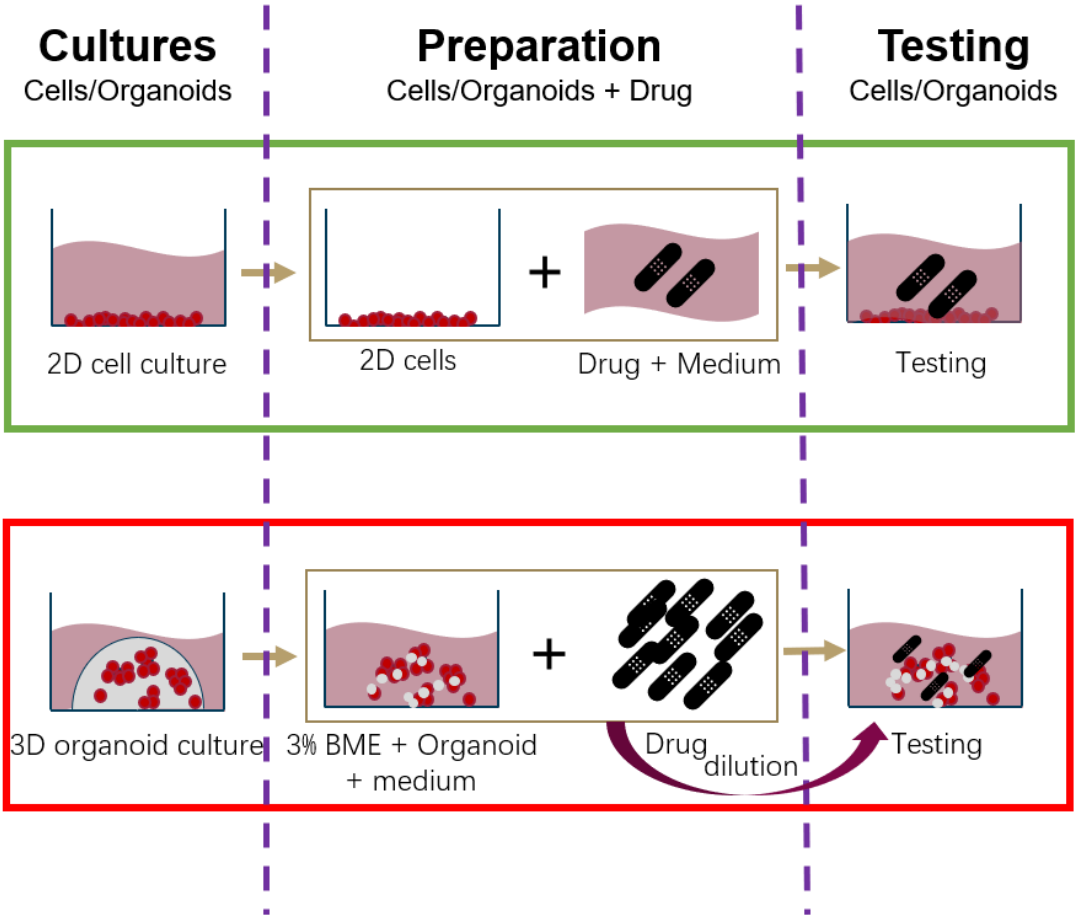

Figure 4: The cytotoxicity assay in CellTiter Glo -3D and -2.0 reagent.

2.20 Data analysis

All data calculations and analyses were performed by a statistical software (GraphPad Prism 8.0) and a spreadsheet program (Microsoft Excel).

3 Results

3.1 Patient derived organoid lines

To establish three-dimension (3D) model of patient derived organoid lines. The UTUC and BC samples were used to establish organoids. We classified 3D cell cultures in BME as organoids after passaging for more than five generations and when they expressed the marker antigens expected for BCO (see below).

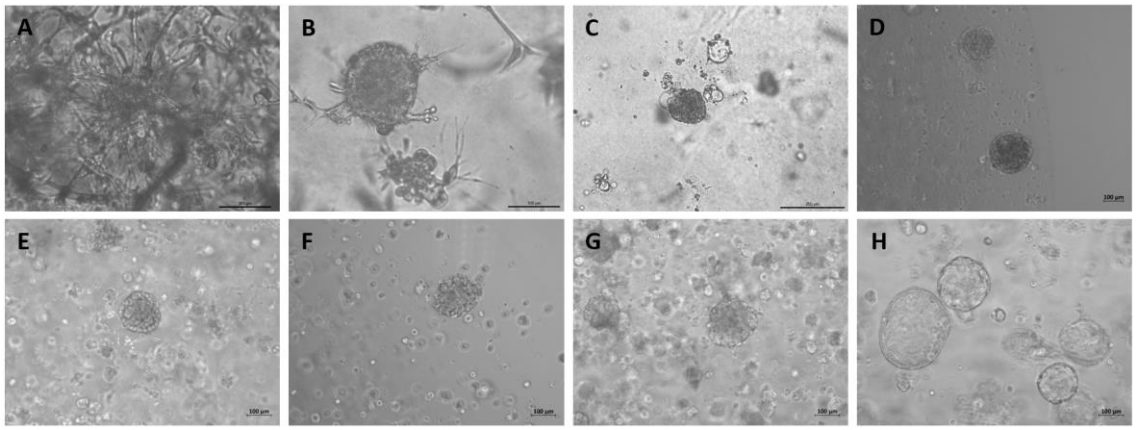

Figure 5: Establishment of organoids after more passaging for more than five generations. A: BCO#41, B: BCO#44, C: RTO#4, D: BCO#107, E: BCO#56, F: BCO#136, G: BCO#140, H: BCO#147. Scale bars indicate 100 µm. The following BCOs were prepared together with Leander Schwaibold and will therefore be also part of his medical thesis: BCO#41, BCO#44, RTO#4, BCO#56.

Each of organoid lines (Figure 5) investigated in this thesis was generated by myself and expanded in HCM medium except BCO#147. The BCO#147 cells were cultured by my colleague who employed a different method to establish and propagate organoids. But I cultured BCO#147 for more than 2 months in HCM medium before doing cytotoxicity assay. In addition, BCO#140 was established in two different methods and cultured in both of HCM and OCM medium, respectively.

Among of them, BCO#41, #44, #107, #136, #140 and RTO#4 were established from BC, and BCO#56 and #147 were generated from UTUC. The ratio of BC to UTUC is 2:6. In

addition, BCO#44 was cultured from a lymphnode metastasis of a bladder cancer. As a variant histology, BCO#140 was a small cell type likely transformed from urothelial cell which described by pathology.

3.2 Characterization of organoids

To characterize organoids, the immunostaining was performed. The sample of UTUC (BCO#56) expressed epithelial and urothelial markers AE1/AE3, CK5, CK8, CK20, as well as FGFR3 and vimentin, which is expressed by mesenchymal cells, the immune modulatory antigen CD47 and the immune checkpoint antigen CD276 (Figure 6). But characterization of the immune checkpoint antigens on organoids was not a key point in my thesis. It therefore was only performed once in the sample of BCO#56. Alexa 488 and Cy3 were used as the negative control.

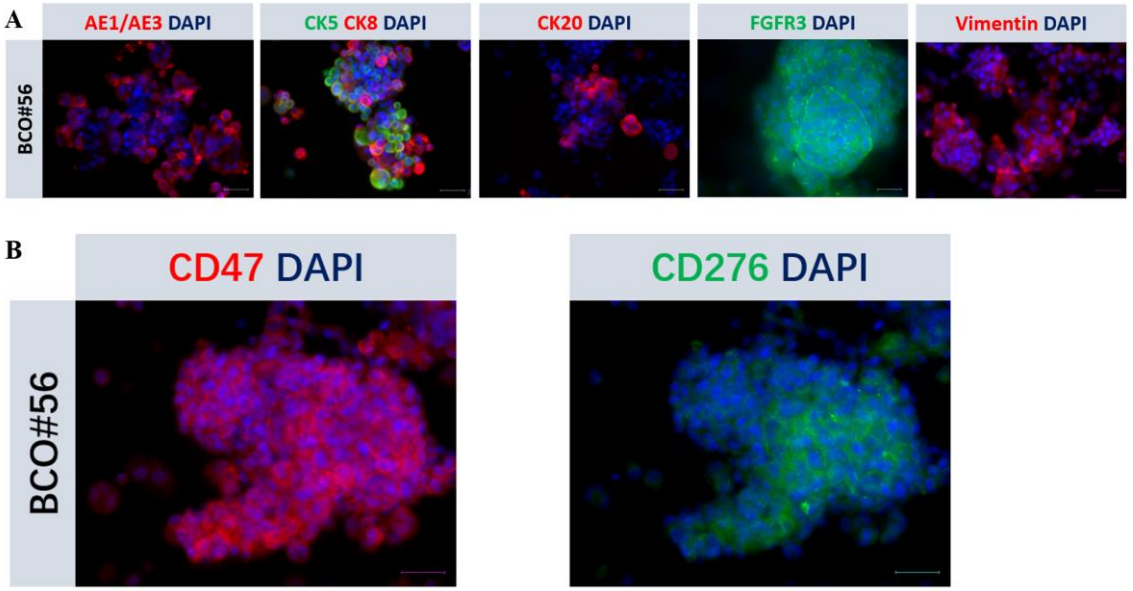

Figure 6: The immunostaining for the organoid lines. (A) Urothelial markers AE1/AE3, CK5, CK8, CK20, FGFR3 and Vimentin were used to characterization upper tract urothelial carcinoma organoid. Scale bars indicate 50μm. (B) Immune checkpoint CD47 and CD276 were detected by upper tract urothelial carcinoma organoid. Scale bars indicate 50 μm.

3.3 Expression of CD47 and CD276 mRNA

A

Experiment: 25-11-2020 CD47_2 and CD276 Yi - 2 Active filter: SYBR Green I / HRM Dye (465-510)

Chart	Pairing	Sample Name	Targets	References	Mean Cp	Mean Cp	Target/Ref	Normalized	Status
True	E1/A1	BCO#56	CD47_2	GAPDH;PPIA		21.92652	0.1107		
True	E2/A2	bmMSC	CD47_2	GAPDH;PPIA	22.20678	24.86621	0.6441		
True	E3/A3	RT4	CD47_2	GAPDH;PPIA	21.19303	23.56471	0.599		
True	E4/A4	HT1197	CD47_2	GAPDH;PPIA	22.2785	23.95279	0.371		
True	E5/A5	HL20/27	CD47_2	GAPDH;PPIA	21.27966	23.19328	0.4706		
True	G1/A1	BCO#56	CD276	GAPDH;PPIA	24.06115	21.92652	0.1304		
True	G2/A2	bmMSC	CD276	GAPDH;PPIA	21.8268	24.86621	2.264		
True	G3/A3	RT4	CD276	GAPDH;PPIA	23.03134	23.56471	0.5622		
True	G4/A4	HT1197	CD276	GAPDH;PPIA	21.0596	23.95279	2.117		
True	G5/A5	HL20/27	CD276	GAPDH;PPIA	22.96707	23.19328	0.4836		

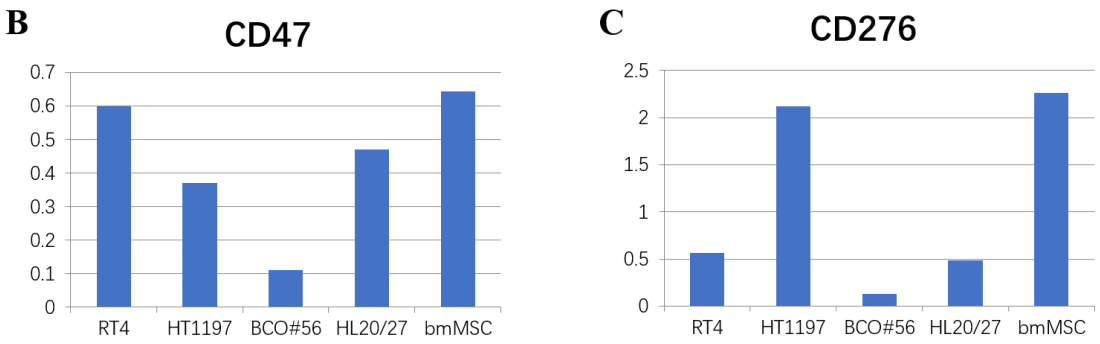

Figure 7: Expression of CD47 and CD276 mRNA in BCO#56 organoid, tumor cell-lines RT4 and HT1197, benign urothelial cells and bmMSC control. GAPDH and PPIA were used as the reference genes. (A) The original data of qRT-PCR from LightCycler 480 System. (B) Expression of CD47 mRNA (C) Expression of CD276 mRNA.

To confirm expression of CD47 and CD276 by organoids and to quantify the expression of CD47 and CD276 mRNA in comparison to normal urothelial cells HL20/27, to the bladder cancer cell lines RT4 and HT1197, and to human bone marrow-derived mesenchymal stromal cells (bmMSCs), the qRT-PCR was performed (Figure 7).

According to the data of qRT-PCR, CD47 and CD276 were expressed in BCO#56 at lower transcript levels than in the tumor cell lines RT4 and HT1197, HL20/27, and bmMSCs. CD276 showed higher expression in RT4 and in bmMSCs than in benign urothelial cells HL20/27. But tumor line HT1197 transcribed less CD276 than HL20/97 (Figure 7).

3.4 Drug response

As organoids are a new experimental cell culture model to investigate drug responses, the classic cytotoxicity WST-assay was used as a reference initially. Then CellTiter-Glo 2.0 reagent was used and compared to WST-assay. At the end, CellTiter-Glo 3D reagent was used to determine the cell viability of cells in 3D organoids and that compared to 2D cells, especially in autologous 2D cell cultures (Figure 8).

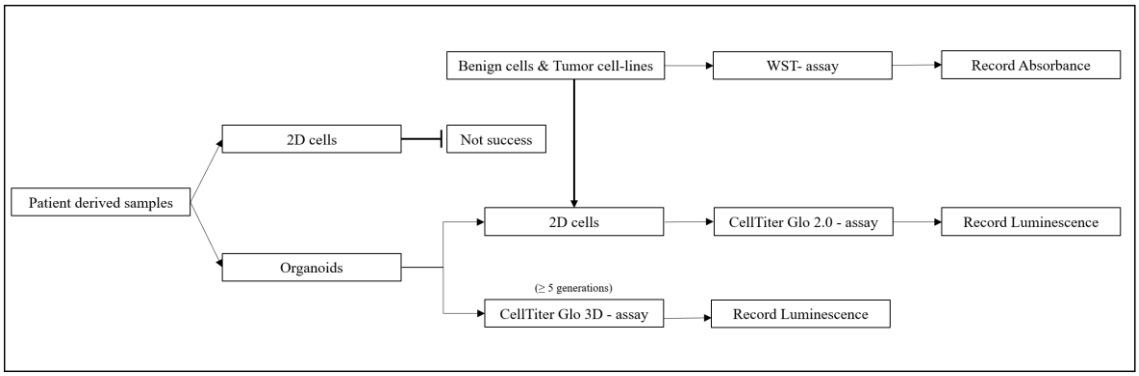

Figure 8: Overview of drug testing plan.

3.4.1 Benign cells and tumor cell-lines

To evaluate the drug response in organoid systems, a conventional 2D cell culture system was used as the reference for it. The IC50s of 2D system were as the comparison value (Table 9).

3.4.1.1 WST-assay

Before evaluation of the drug responds, the suitable drug testing concentrations should be titrated. Initially, each drug was tested in 6 different concentrations: For titration of Cisplatin the following concentrations were used: 66µM, 33µM, 25µM, 12.5µM, 6.25µM, 3.125µM and 1.5625µM. Venetoclax and S63845 belong to the Bcl-2 family of inhibitors. We therefore used these two drugs at the same concentrations to evaluate and

compare drug responses. Venetoclax was used at the following concentrations: 25µM, 10µM, 4µM, 1.6µM, 0.64µM, 0.256µM and 0.1024µM ((Figure 9).

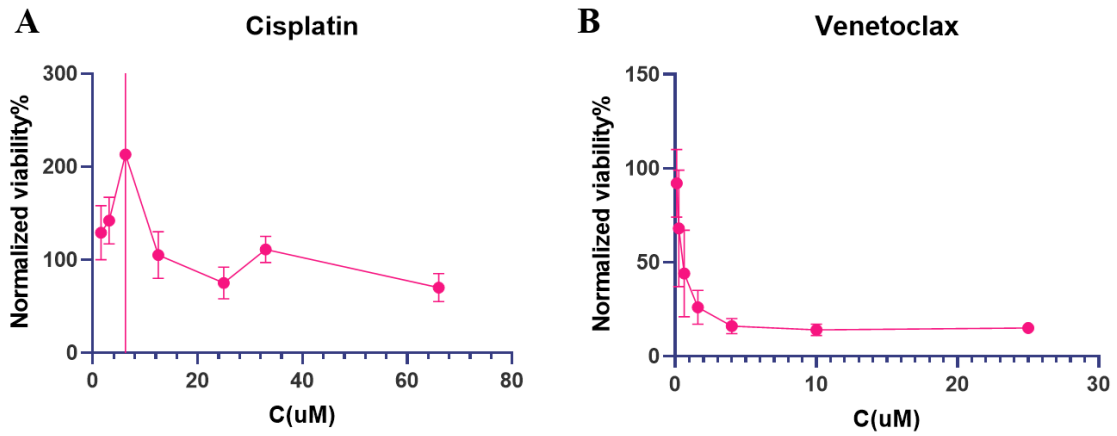

Figure 9: Cytotoxicity assay by WST reagent. (A) The normalized cell viability of Cisplatin. Treatment concentrations of cisplatin were 66µM, 33µM, 25µM, 12.5µM, 6.25µM, 3.125µM and 1.5625µM, respectively. (B) Normalized cell viability of Venetoclax. The treatment concentrations of Venetoclax were 25µM, 10µM, 4µM, 1.6µM, 0.64µM, 0.256µM and 0.1024µM, respectively.

After initial drug titration, in the actual experiments the following drug concentrations were used: Cisplatin at 30µM, 10µM, 3µM and 1µM to evaluate the drug response. Venetoclax and S63845 at 25µM, 10µM, 4µM and 1.6µM.

In addition, the appropriate cell inoculation densities and cell growth conditions must be determined, to obtain a sufficient read-out after short incubation times and consistent time- and dose-dependent results during follow-up. 5.000 cells/well and 10,000 cells/well were initially used. Under these two cell concentrations, RT4 and HT1197 cell-lines were treated by cisplatin, venetoclax and S63845 for 24 hours, 48 hours, 72 hours and 96 hours (Figure 10). These conditions granted consistent results.

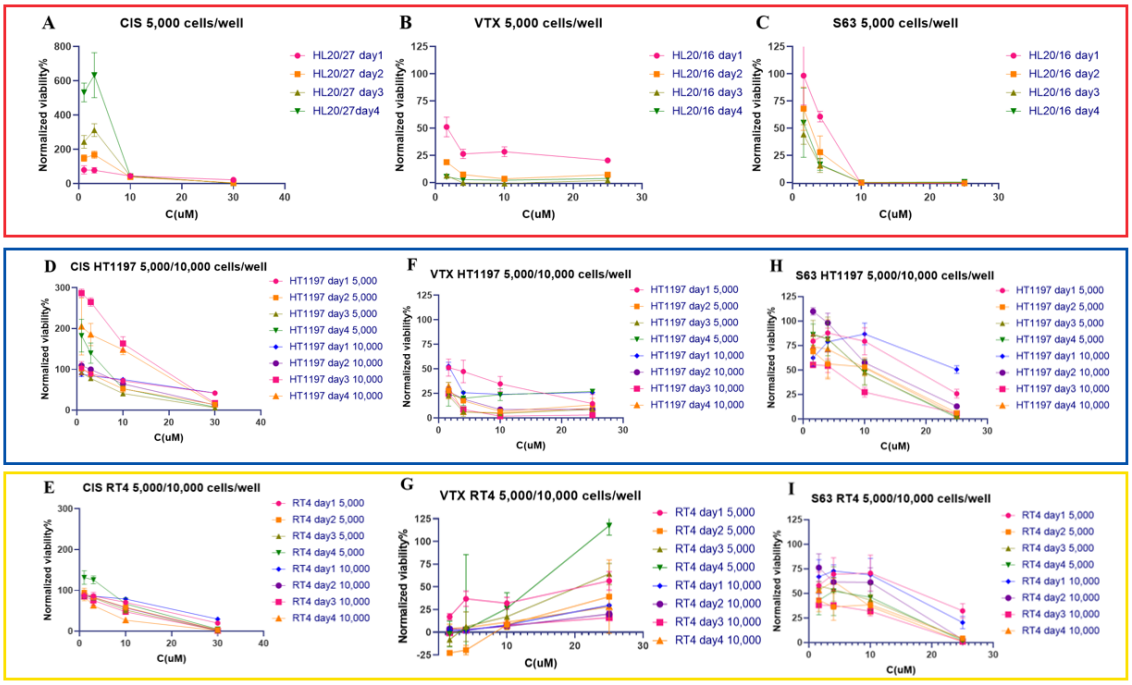

Figure 10: WST-assay in Cisplatin, Venetoclax and S63845 towards benign urothelial cells, RT4 and HT1197 cell-lines. 30µM, 10µM, 3µM and 1µM were used in Cisplatin. 25µM, 10µM, 4µM and 1.6µM were treated by Venetoclax and S63845. (A, B, C) The benign urothelial cells were used in 5,000 cells/96-well and tested for 24h, 48h, 72h and 96h. (D, F, H) HT1197 cell-lines in 5,000 and 10,000 cells/96-well were performed to determine the cell viabilities in 24h, 48h, 72h and 96h. (E, G, I) The same methods as HT1197 were performed to evaluate cell viabilities of RT4 cell-lines as well.

3.4.1.2 CellTiter Glo-2.0 assay

Complementary to the WST-assay, analyses with the reagent CellTiter Glo-2.0 were performed to evaluate the sensitivity and reproducibility of the cell viability tests included in this study (Figure 11). Because the testing values of 3D organoids can be recorded only by luminescence (but not by MTT-like chemistry) we used the CellTiter Glo-2.0 in 2D cultures versus Glo-3.0 chemistry for organoids.

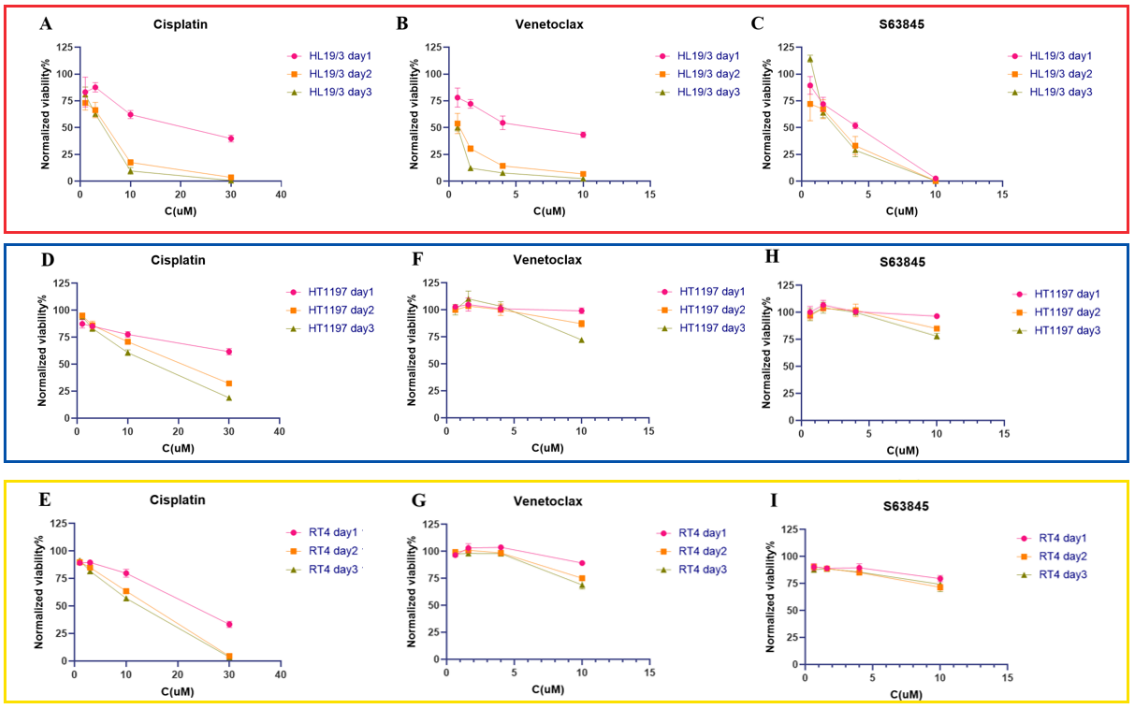

Figure 11: CellTiter Glo 2.0 assay in Cisplatin, Venetoclax and S63845 towards benign urothelial cells, RT4 and HT1197 cell-lines in 24h, 48h and 72h. (A, B, C) The normalized cell viability of benign cells was determined by cisplatin, venetoclax and s63845 in 24h, 48h and 72h, respectively. (D, E), (F, G), (H, I) The normalized cell viability of HT1197 and RT4 cell-lines were tested by cisplatin, venetoclax and s63845 in 24h, 48h and 72h, respectively.

	Benign		HT1197		RT4	
IC_{50} (μM)	WST	CellTiter Glo 2.0	WST	CellTiter Glo 2.0	WST	CellTiter Glo 2.0
Cisplatin day1	8.41	19.01	22.38	91.56	18.85	20.45
Cisplatin day2	~9.71	3.67	10.50	17.76	10.06	11.82
Cisplatin day3	~9.83	3.52	7.184	12.05	7.27	9.96
Cisplatin day4	-	/	~10.05	/	4.31	/
Venetoclax day1	1.18	6.21	2.378	~252423	41.88	~11.76
Venetoclax day2	0.21	0.74	4.633e+150	~12.16	85.27	13.70
Venetoclax day3	6.143e+152	0.63	0.38	~10.71	113.6	12.78
Venetoclax day4	6.176e+150	/	19787407	/	60.42	/
S63845 day1	~4.15	3.29	16.26	~12.05	10.81	755.7
S63845 day2	2.37	2.12	5.48	~11.51	7.24	59.68
S63845 day3	2.290e+151	2.41	8.62	~11.49	5.011e+143	195.00
S63845 day4	1.77	/	8.59	/	3.57	/

Table 9: The IC50s of cisplatin, venetoclax and s63845 from WST and CellTiter Glo-2.0 assay in benign urothelial cells and tumor cell-lines. "-" means not converged (analysis by GraphPad Prism 8). "/" means not test.

3.4.2 Drug testing by patient derived organoid and autologous 2D cells

Patient derived organoids and the corresponding 2D cells were treated by cisplatin, venetoclax and S63845, respectively. Records of the luminescence generated after 24h, 48h and 72h of incubation were used to calculate the cell viabilities (Figure 12, 13, 14). The IC50s (Table 10) of them were analysed by GraphPad Prism 8. For BCO#147 not enough organoids and corresponding 2D cells were available due to reduced cell growth when the testing was performed. We therefore only chose to record the results in day 3 with BCO#147.

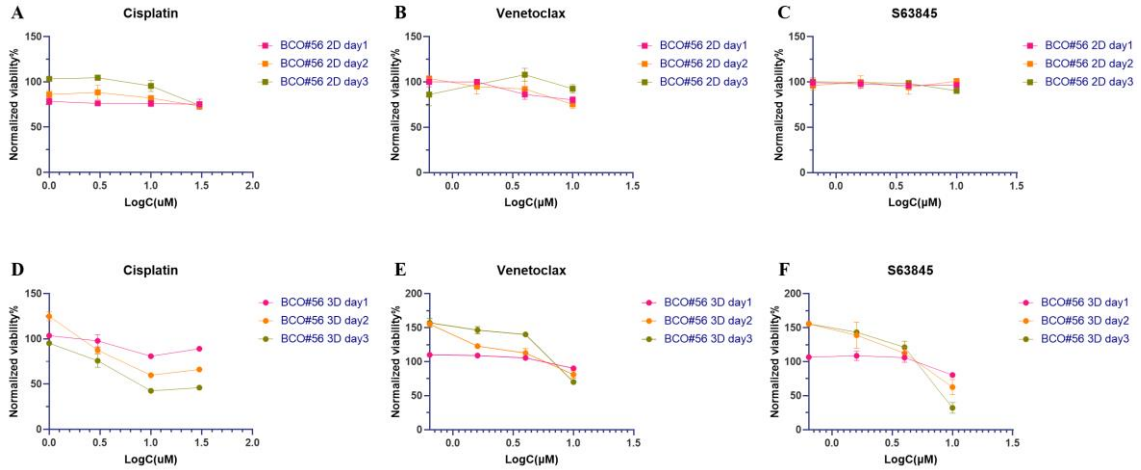

Figure 12: The normalized cell viability in: BCO#56. (A, B, C) The normalized cell viability in 2D cell cultures towards to cisplatin, venetoclax and S63845 in 3 days. (D, E, F) In 3D organoids of normalized cell viabilities towards to CIS, VTX and S63 in 3 days.

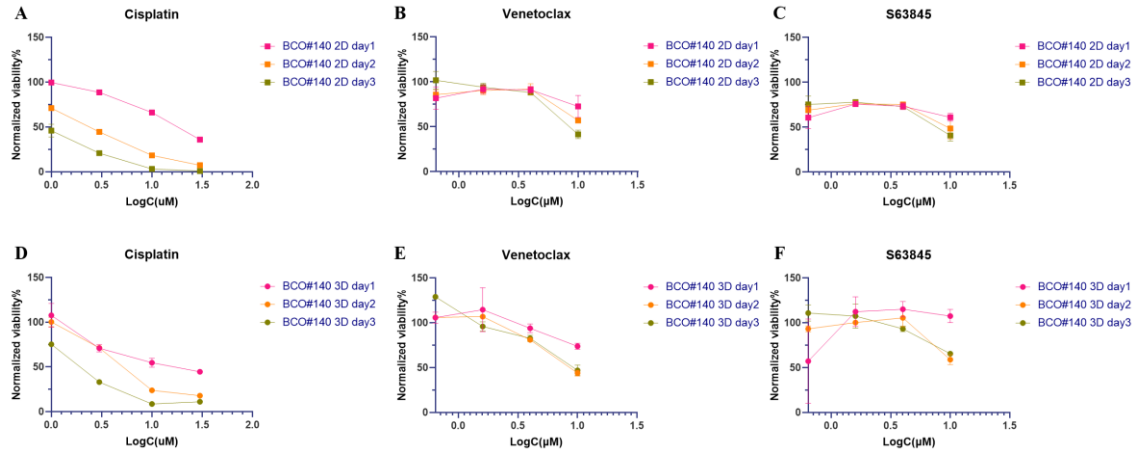

Figure 13: The normalized cell viabilities in BCO#140. (A, B, C) The cell viabilities towards to cisplatin, venetoclax and S63845 in 2D cell cultures in 3 days. (D, E, F) In 3D organoids of normalized cell viabilities towards to CIS, VTX and S63 in 3 days.

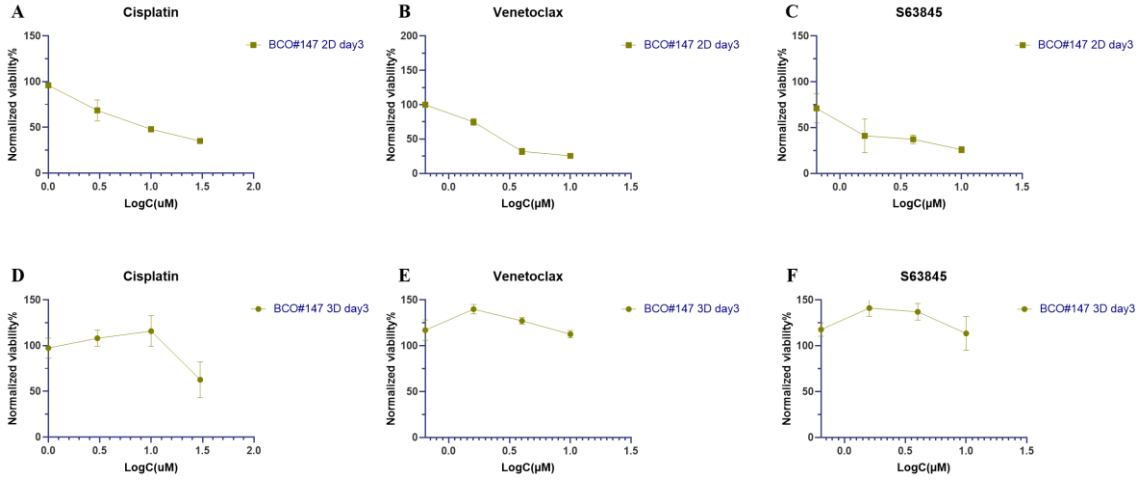

Figure 14: The normalized cell viabilities of BCO#147 in day 3. (A, B, C) In 2D cell cultures of cell viabilities towards to CIS, VTX and S63. (D, E, F) In 3D organoids of normalized cell viabilities towards to CIS, VTX and S63.

	BCO#56		BCO#140		BCO#147	
IC_{50} (μM)	2D	3D	2D	3D	2D	3D
Cisplatin day1	-	799.2	18.08	16.90	/	/
Cisplatin day2	1052	42.93	2.40	5.23	/	/
Cisplatin day3	49.82	15.48	0.89	1.99	10.85	~31.31
Venetoclax day1	36.39	~11.15	388.1	14.74	/	/
Venetoclax day2	21.88	~10.79	12.74	8.78	/	/
Venetoclax day3	0.32	~10.41	8.733	9.27	3.152	~2.986e+048
S63845 day1	124397	~11.08	-	~0.63	/	/
S63845 day2	9.206e-005	~10.25	21.34	~10.11	/	/
S63845 day3	29.77	~9.53	8.88	12.79	1.63	~

Table 10: The IC50s of cisplatin, venetoclax and S63845 in 2D cell cultures and organoids. "-" means interrupted, IC50s=0 (analysis by GraphPad Prism 8). "/" means not test. " ~ " means high.

To compare the results of organoids and 2D cell cultures with the same situation, only results obtained on day 3 were explored to evaluate the effects of these drugs (Figure 15).

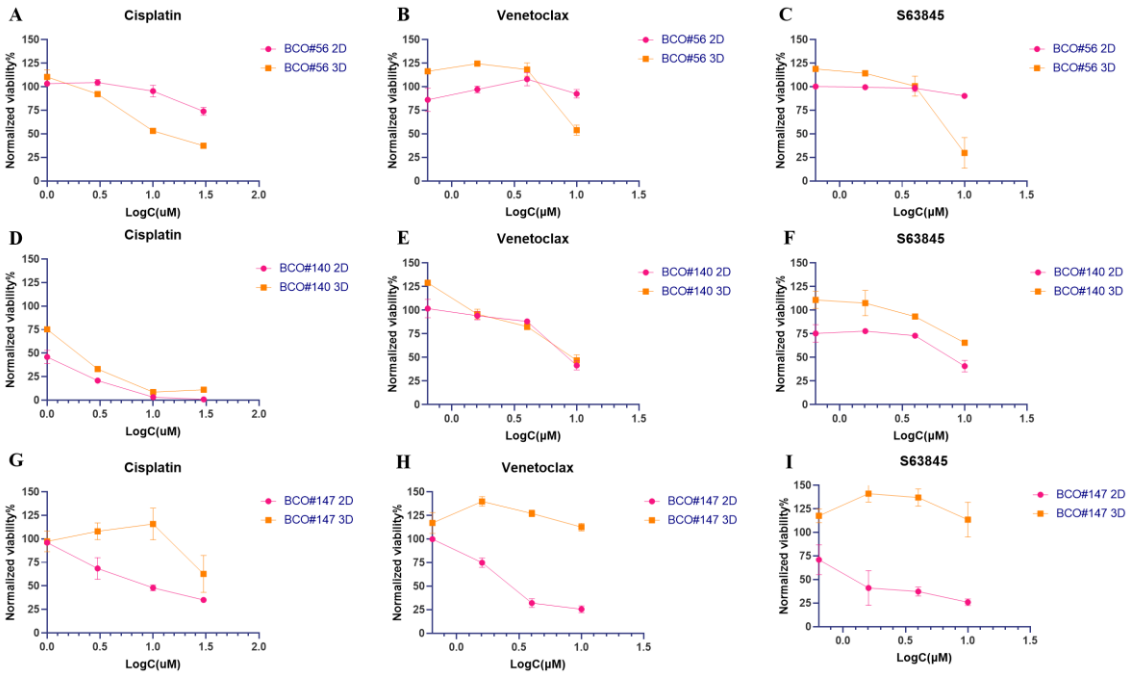

Figure 15: Comparison normalized cell viabilities in organoids and autologous 2D cell cultures. (A, B, C), (D, E, F), (G, H, I) Cell viabilities of cisplatin, venetoclax and s63845 in 3D organoids and autologous 2D cell cultures in BCO#56, BCO#140 and BCO#147, respectively.

3.4.3 Comparison organoids, autologous 2D cell cultures and standard cells

The cytotoxicity assay was tested by WST and CellTiter Glo 2.0/3D reagent. The WST reagent was recorded by absorbance, but CellTiter Glo 2.0/3D reagent were recorded by luminescence. To evaluate the drug response between 2D cell cultures and 3D organoids system, the unitary conditions was necessary. Therefore, we performed 2D cells versus 3D organoids in the luminescence assay. To compare them clearly, the curve of 2D cells assay were merged together to compared to 3D organoids (Figure 16). The IC50s of cytotoxicity assay in 2D and 3D were shown in the (Table 9,10.).

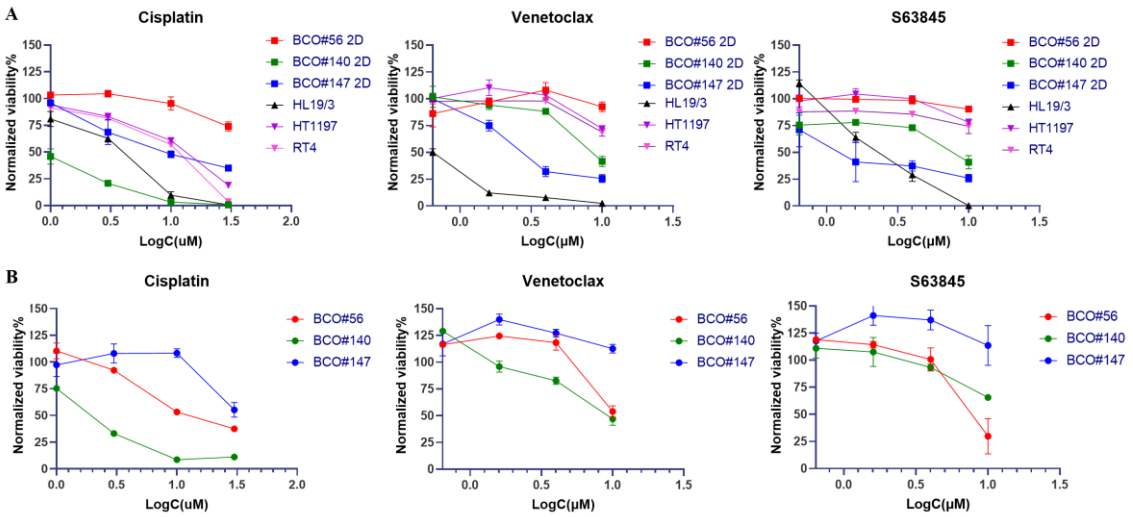

Figure 16: The normalized cell viabilities in 2D normal cells, tumor cell-lines, organoids and autologous 2D cell cultures. (A) Cell viabilities in 2D benign urothelial cells, tumor cell-lines and patient derived 2D cell cultures. (B) Cell viabilities from patient derived organoids.

4 Discussion

4.1 Establishment and characterization of organoids

Based on the current state-of-the-art, production of patient-derived BC and UTUC origin, has been brought to the research laboratories of Dept. of Urology at UKT. The groundbreaking technical work how to generate BCO had been established by other research groups recently (Lee SH et al. 2018; Mullenders J et al. 2019). However, they generated organoids from non-muscle invasive bladder cancer or muscle invasive bladder cancer. In contrast, to the best of our knowledge we describe for the first-time upper tract urothelial cell carcinoma organoids. Experts agreed that 3D constructs should be named organoids when they are consecutively passaged at least six times (Lee SH et al. 2018). Others used the term organoid after only a few days of culture but propagated these organoids for more than 1 year (Mullenders J et al. 2019). In addition, (Pauli C et al. 2017) reported multiple organoid cultures from 18 different tumor types, including bladder/ureter, and defined organoids as spheroid-like structures and passaged them at least 5 times. In our study, organoids were defined as spheroid cultures after passaging for more than 5 generations followed by cellular characterization. Our first organoid line BCO#56 was passaged to reach in consecutive culture 33 passages and 2 years of continued growth.

Before applications of organoids can be planned one of the most important prerequisites was to easily to generate them. According to the results of (Lee SH et al. 2018), bladder cancer organoids were generated in 12 out of 17 samples within 9 months. Based on (Mullenders J et al. 2019), 77 of organoid lines were established from 133 tissue samples derived from tissue samples of 53 patients, including normal tissue- and tumor-derived organoids. (Pauli C et al. 2017) showed that 56 organoids were generated from 145 surgical samples. In our lab, in the past 2 years, urothelial carcinoma organoids were generated from 107 patient samples using our protocols and our criteria for quality

controls. Overall, the success rate was less than 10%. In order to improve the situation, two different expansion media, HCM and OCM, (Table 4) were used to culture organoids and improve the success rate. OCM medium showed a better culture efficacy than HCM medium in early organoid cultures, i.e., before 2-3 generations. However, OCM medium hardly supported growth of organoids for a longer period exceeding 5 generations. In contrast, HCM medium after two- or three-weeks of culture, showed better organoid morphology and supported growth of organoids in higher passages. Because higher success rates can be achieved by employing HCM medium in organoid cultures, we decided to use preferably HCM medium to establish organoid lines in this study. However, it might be possible to further rise the success rates of organoid cultures when using yet different media during different time intervals. Studies along these lines are currently under way. The organoid culture of urothelial carcinoma cells and their application in urology are still in an early stage of research. Therefore, the rate of success in organoid culture should be evaluated objectively.

Several of the organoid cultures grew initially well but failed to proliferate when they reached 6-7 passages. These cultures died gradually after 1-2 months of growth. Due to the limited number of lines available during this study, we couldn't investigate the reasons for culture failure. But some specificities of the tumor tissues obtained (figure 17), including limited weight and size, surgical techniques applied to prepare the samples (e. electrocautery vs. removal by blade), lack of sufficient numbers tumor (stem-) cells when passaging generation after generation might be some relevant reasons for loss of the organoids in early stages of culture.

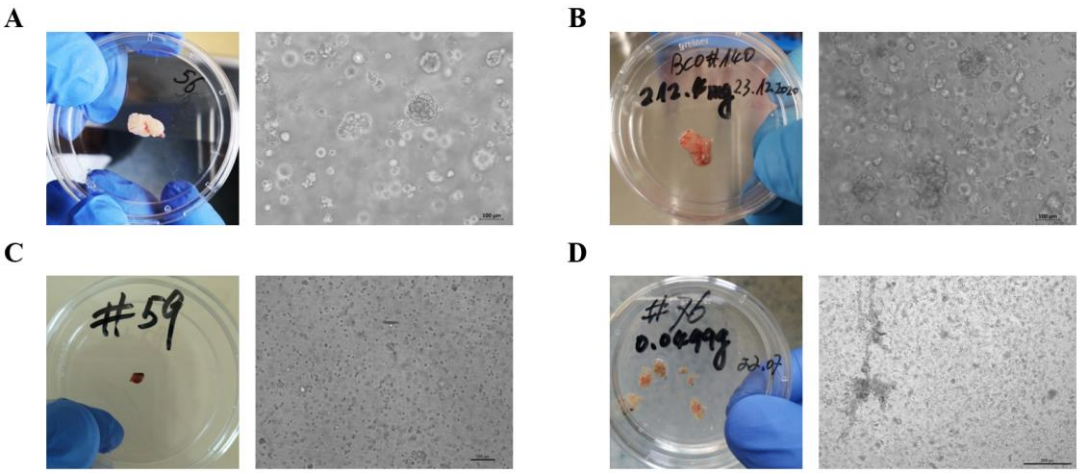

Figure 17: Tumor tissues and autologous images in microscope. (A, B) These two samples were generated the best organoid lines. (C, D) These two tissues were failed to establish organoids.

So far, human tissue-derived organoids have been established from intestinal (Sato T et al. 2011), liver (Takebe T et al. 2013), brain (Lancaster MA et al. 2013), gastric (McCracken KW et al. 2014), lung (Dye BR et al. 2015), pancreatic (Boj SF et al. 2015), renal (Takasato M et al. 2015) thyroid (Kurmann AA et al. 2015) and other tissues. But up to now tumor-derived organoids can't be generated currently from just any tissue source (Lancaster MA et al. 2019). When progress on tissue- or tumor-derived organoids from different tissues was published, some of the establishment methods presented organoids with an interesting appearance. (Boretto M et al. 2017 and Turco MY et al. 2017) reported endometrial organoids established through a mimetic condition which appeared like liver organoids (Lancaster MA et al. 2019), and (Kessler M et al. 2015) described a method, which contained many similar steps compared to production of gastric organoid to generate fallopian tube organoids (Barker N et al. 2010). The similar experience also happened in our study. Employing the same methods and culture medium, which were published for production of urothelial carcinoma organoids, we were capable to maintain breast cancer organoids which appeared very closely related to the 3D constructs described originally (Gudjonsson T et al. 2002; Linnemann JR et al. 2015). The reasons for this finding might be that the cultures media applied are not highly selective for unique organ. Or the molecular subtypes between bladder and breast cancer

cells share some similarities with respect to nutritial need and expression of biomarkers, such as basal (cytokeratin 5) and luminal (cytokeratin 20) subtypes. These two types of tumors might be similar in some aspects on the molecular level (Damrauer JS et al. 2014; Perou CM et al. 2000; Choi W et al. 2014).

In our research, each organoid expressed urothelial marker AE1/AE3, cytokeratin 5 (basal) and cytokeratin 20 (luminal), the potential therapeutic target FGFR3 (van Rhijn BW et al. 2014), and the immune modulatory molecules CD276 and CD44, respectively. In addition, expression of the mesenchymal antigen vimentin was observed in organoids in vitro. Organoids were highly recapitulating the features of tumors in vitro. Interestingly, in BCO#147 (in the research by Nizar Lipke), the expression of luminal CK 20 was recorded only in an individual organoid, but the others organoids which were close to it did not express any marker protein. This indicated distinct differentiation or maturation of cells in individual organoids. In addition, the results of qRT-PCR presented an interesting difference in expression of checkpoint antigen CD276 and immune modulatory CD44 between organoids and cells. We can say organoid lines always maintain the independent features, which were different from our predictions. These reasons might be because of organoids always contains highly cellular plasticity and tumor heterogeneity (Lee SH et al. 2018); Choi W et al. 2014) in vitro environment.

4.2 Drug responses

To investigate the drug response in organoids, we divided our cytotoxicity assay in 3 study arms: 1) A WST-assay (absorbance) was used to detected cell viabilities of benign urothelial cells and tumor cell lines towards Cisplatin, Venetoclax and S63845 after 4 days of incubation in adherent 2D cultures. 2) CellTiter Glo 2.0-assays (luminescence) were performed to evaluate the cell viabilities of benign urothelial cells, tumor cell lines and patient derived tumor cells towards to Cisplatin, Venetoclax and S63845 after 3 days

of incubation in adherent 2D cultures. 3) CellTiter Glo 3D-assays (luminescence) were performed to evaluate the cell viabilities of organoid lines towards to Cisplatin, Venetoclax and S63845 after 3 days of incubation of organoids. The well-established absorbance-assay (WST) was used primarily as a reference to establish the novel luminescence-assay (CellTiter Glo 2.0) system in 2-dimonsional (2D) cell cultures system in our laboratory. The cell viabilities in 2D cell cultures were then used to as the reference for 3D organoids. To better understand and compare the effects of different drugs in 2D cell cultures versus 3D organoids, we chose the value of IC50s and the time point day 3 to evaluate drug response.

After testing, 2D and 3D systems revealed corresponding results in the two different absorbance- and luminescence-assays, and IC50s in 2D cells were confirmed in a fair range when compared to previously published data (https://www.cancerrxgene.org/celllines). These results showed in independent tests a correlation to each other. Therefore, the novel 2D GloMax assay was considered a robust method. However, in 2D cell cultures system, the luminescence-assay showed higher sensitivity than the absorbance-assay, because in luminescence-assay demonstrated unambiguously different IC50s of Cisplatin between benign urothelial and tumor cells but presented almost close value when compared by the absorbance-assay (Table 9). In addition, luminescence-assay might be more stable to evaluate the drug response than absorbance-assay according to the range of IC50s between benign and tumor cells towards to Venetoclax and S63845. We therefore recommend the luminescence-assay as the priority test to detect the IC50s of novel drugs rather than absorbance-assay.

When we compared benign urothelial and tumor cells in the luminescence-assay, benign urothelial cells showed higher sensitivities to Venetoclax and S63845 compared to Cisplatin, RT4 cell lines showed lower sensitivity to Cisplatin, specifically with significantly different towards S63845. In other words, the RT4 cell-line was sensitive to

the BCL-2 inhibitor (VTX) but resistant to MCL-1 inhibitor (S63). This may be because the RT4 cell-line is BCL-2-dependent, and only BCL-2-dependent cells can be targeted by Venetoclax (Villalobos-Ortiz M et al. 2020). In the bladder cancer line HT1197, Cisplatin presented similar effects as the two other compounds (Table 9).

Comparably, in our study the IC50s of the three samples of patient-derived 3D organoids and autologous 2D cell cultures demonstrated individual responses in drug testing. In BCO#56, an organoid with upper tract urothelial carcinoma origin, both the 3D and corresponding 2D cultures were significantly more sensitive towards Venetoclax and S63845 when compared to cisplatin sensitivities. Interestingly, 2D cells of BCO#56 presented clearly significantly more sensitive to Venetoclax (BCL-2 inhibitor) but were resistant to S63845 (MCL-1 inhibitor). However, the corresponding organoids showed very similar effects with Venetoclax and S63845. This indicated that organoid analyses might be a new way to evaluate the effect of these drugs, that are currently not used to treat urothelial cancer. In BCO#140, Cisplatin generated higher sensitivities than Venetoclax and S63845 in 2D and 3D system. But they showed almost the same IC50s of Venetoclax and S63845 between organoids and corresponding cells. In BCO#147, Cisplatin, Venetoclax and S63845 testing of organoids yielded lower sensitivity than the autologous 2D cells. Interestingly, BCO#147 organoids were significantly more inert than the corresponding 2D cell cultures system towards Venetoclax and S63845. It seems that in BCO#147 mitochondria- mediated apoptotic pathways respond to these components only in 2D systems, but not in 3D organoids. Molecular analyses exploring these differences must await future experiments.

The sensitivity of BC and UTUC towards Cisplatin, Venetoclax and S63845 differed substantially, depending on whether it was assessed in conventional 2D cell culture or novel 3D organoids. Further research is needed to determine if conventional 2D cell cultures or newer 3D organoids are the more reliable method for assessing cytotoxicity in

vitro. Until then, results from both methods should considered and included in pre-clinical studies, unless one method is consistent with results from the other method. In addition, due to the fact that in vitro data include not all effects when compared to in vivo responses, more pre-clinical research could be performed and correlated with the response of individual patients in the future.

5 Summary

5.1 Summary in English

Cancer is a major health problem around the world. Among all cancer cases, urothelial carcinomas (UCs) were the 6th most common cancer in the records in 2021 in developed countries, and the prognosis of UCs is still in a poor situation. Therefore, we need a model which can better recapitulate the disease to improve this situation, rather than only focus on conventional cell-lines or animal models. In past several decades, more and more in vitro disease models have been explored. In this context, the 3-dimentional (3D) organoid culture system is highlighted as a novel key technology in cancer research. Organoids offer a way to explore in vitro the interplay of the tumor and its microenvironment under conditions much closer to the in vivo situation than conventional 2D cell cultures. In this study, we generated a method to establish patient-derived organoid model of the UCs (UTUCs and BC) and characterized them by antibodies AE1/AE3, and against CK 5, CK 8, CK 20, FGFR3 and vimentin. In addition, to test the drug response of this 3D organoid model, a cytotoxicity assay was performed in 3D organoids and autologous conventional 2D cells towards Cisplatin, Venetoclax and S63845. We report significant differences in cytotoxicity results between 2D versus 3D cultures. The limitations of this study include the low number of individual patient samples and the lack of assays in very early-stage organoids in comparison to later stage cultures. We conclude that further research is needed to determine if conventional 2D cell culture or newer 3D organoids are the more reliable method for assessing cytotoxicity in vitro.

5.2 Zusammenfassung

Krebs ist weltweit ein großes Gesundheitsproblem. Unter allen Krebsfällen waren Urothelkarzinome (UCs) im Jahr 2021 die sechsthäufigste Krebserkrankung in den Aufzeichnungen und die Prognose von UCs ist immer noch schlecht. Daher brauchen wir ein Modell, das der Krankheit besser entspricht, um diese Situation zu verbessern, anstatt sich nur auf konventionelle Zelllinien oder Tiermodelle zu konzentrieren. In den letzten Jahrzehnten wurden immer mehr in-vitro-Krankheitsmodelle erforscht. In diesem Zusammenhang wird das 3-dimensionale (3D) organoide Kultursystem als neuartige Schlüsseltechnologie in der Krebsforschung hervorgehoben. Organoide bieten eine Möglichkeit, das Zusammenspiel des Tumors und seiner Mikroumgebung in vitro unter Bedingungen zu untersuchen, die der in vivo-Situation viel näherkommen als herkömmliche 2D-Zellkulturen. In dieser Studie entwickelten wir eine Methode zur Etablierung von Patienten abgeleiteten Organoidmodellen der UCs aus dem oberen Harntrakt (UTUCs) und aus der Blase (BC) und charakterisierten sie durch Antikörper AE1/AE3 und die gegen CK5, CK8, CK20, FGFR3 und Vimentin. Um die Arzneimittelantwort dieses 3D-Organoidmodells zu testen, wurde ein Zytotoxizitätsassay in 3D-Organoiden im Vergleich zu konventionellen 2D-Zellen desselben Patienten gegenüber Cisplatin, Venetoclax und S63845 durchgeführt. Wir berichten über signifikante Unterschiede in den Zytotoxizitätsergebnissen zwischen 2D- und 3D-Kulturen. Zu den Einschränkungen dieser Studie zählen die geringe Anzahl individueller Patientenproben und das Fehlen von Assays von Organoiden in sehr frühen Stadien im Vergleich zu Kulturen in späteren Stadien. Wir schließen daraus, dass weitere Forschung erforderlich ist, um festzustellen, ob konventionelle 2D-Zellkulturen oder neuere 3D-Organoide die zuverlässigere Methode zur Bewertung der Zytotoxizität in vitro sind.

6 Bibliography

AICHER, W. K., KORN, M., REITNAUER, L., MAURER, F. B., HENNENLOTTER, J., BLACK, P. C., TODENHOFER, T., BEDKE, J. & STENZL, A. 2021. Expression patterns of the immune checkpoint ligand CD276 in urothelial carcinoma. *BMC Urol,* 21**,** 60.

BARKER, N., HUCH, M., KUJALA, P., VAN DE WETERING, M., SNIPPERT, H. J., VAN ES, J. H., SATO, T., STANGE, D. E., BEGTHEL, H., VAN DEN BORN, M., DANENBERG, E., VAN DEN BRINK, S., KORVING, J., ABO, A., PETERS, P. J., WRIGHT, N., POULSOM, R. & CLEVERS, H. 2010. Lgr5(+ve) stem cells drive self-renewal in the stomach and build long-lived gastric units in vitro. *Cell Stem Cell,* 6**,** 25-36.

BARTFELD, S., BAYRAM, T., VAN DE WETERING, M., HUCH, M., BEGTHEL, H., KUJALA, P., VRIES, R., PETERS, P. J. & CLEVERS, H. 2015. In vitro expansion of human gastric epithelial stem cells and their responses to bacterial infection. *Gastroenterology,* 148**,** 126-136 e6.

BEN-DAVID, U., SIRANOSIAN, B., HA, G., TANG, H., OREN, Y., HINOHARA, K., STRATHDEE, C. A., DEMPSTER, J., LYONS, N. J., BURNS, R., NAG, A., KUGENER, G., CIMINI, B., TSVETKOV, P., MARUVKA, Y. E., O'ROURKE, R., GARRITY, A., TUBELLI, A. A., BANDOPADHAYAY, P., TSHERNIAK, A., VAZQUEZ, F., WONG, B., BIRGER, C., GHANDI, M., THORNER, A. R., BITTKER, J. A., MEYERSON, M., GETZ, G., BEROUKHIM, R. & GOLUB, T. R. 2018. Genetic and transcriptional evolution alters cancer cell line drug response. *Nature,* 560**,** 325-330.

BERKERS, G., VAN MOURIK, P., VONK, A. M., KRUISSELBRINK, E., DEKKERS, J. F., DE WINTER-DE GROOT, K. M., ARETS, H. G. M., MARCK-VAN DER WILT, R. E. P., DIJKEMA, J. S., VANDERSCHUREN, M. M., HOUWEN, R. H. J., HEIJERMAN, H. G. M., VAN DE GRAAF, E. A., ELIAS, S. G., MAJOOR, C. J., KOPPELMAN, G. H., ROUKEMA, J., BAKKER, M., JANSSENS, H. M., VAN DER MEER, R., VRIES, R. G. J., CLEVERS, H. C., DE JONGE, H. R., BEEKMAN, J. M. & VAN DER ENT, C. K. 2019. Rectal Organoids Enable Personalized Treatment of Cystic Fibrosis. *Cell Rep,* 26**,** 1701-1708 e3.

BOJ, S. F., HWANG, C. I., BAKER, L. A., CHIO, II, ENGLE, D. D., CORBO, V., JAGER, M., PONZ-SARVISE, M., TIRIAC, H., SPECTOR, M. S., GRACANIN, A., ONI, T., YU, K. H., VAN BOXTEL, R., HUCH, M., RIVERA, K. D., WILSON, J. P., FEIGIN, M. E., OHLUND, D., HANDLY-SANTANA, A., ARDITO-ABRAHAM, C. M., LUDWIG, M., ELYADA, E., ALAGESAN, B., BIFFI, G., YORDANOV, G. N., DELCUZE, B., CREIGHTON, B., WRIGHT, K., PARK, Y., MORSINK, F. H., MOLENAAR,

I. Q., BOREL RINKES, I. H., CUPPEN, E., HAO, Y., JIN, Y., NIJMAN, I. J., IACOBUZIO-DONAHUE, C., LEACH, S. D., PAPPIN, D. J., HAMMELL, M., KLIMSTRA, D. S., BASTURK, O., HRUBAN, R. H., OFFERHAUS, G. J., VRIES, R. G., CLEVERS, H. & TUVESON, D. A. 2015. Organoid models of human and mouse ductal pancreatic cancer. *Cell,* 160**,** 324-38.

BORETTO, M., COX, B., NOBEN, M., HENDRIKS, N., FASSBENDER, A., ROOSE, H., AMANT, F., TIMMERMAN, D., TOMASSETTI, C., VANHIE, A., MEULEMAN, C., FERRANTE, M. & VANKELECOM, H. 2017. Development of organoids from mouse and human endometrium showing endometrial epithelium physiology and long-term expandability. *Development,* 144**,** 1775-1786.

BRAUSI, M., COLLETTE, L., KURTH, K., VAN DER MEIJDEN, A. P., OOSTERLINCK, W., WITJES, J. A., NEWLING, D., BOUFFIOUX, C. & SYLVESTER, R. J. 2002. Variability in the recurrence rate at first follow-up cystoscopy after TUR in stage Ta T1 transitional cell carcinoma of the bladder: a combined analysis of seven EORTC studies. *Eur Urol,* 41**,** 523-31.

BRUNELLE, J. K., RYAN, J., YECIES, D., OPFERMAN, J. T. & LETAI, A. 2009. MCL-1-dependent leukemia cells are more sensitive to chemotherapy than BCL-2-dependent counterparts. *J Cell Biol,* 187**,** 429-42.

CHAE, Y. K., RANGANATH, K., HAMMERMAN, P. S., VAKLAVAS, C., MOHINDRA, N., KALYAN, A., MATSANGOU, M., COSTA, R., CARNEIRO, B., VILLAFLOR, V. M., CRISTOFANILLI, M. & GILES, F. J. 2017. Inhibition of the fibroblast growth factor receptor (FGFR) pathway: the current landscape and barriers to clinical application. *Oncotarget,* 8**,** 16052-16074.

CHEN, K. G., MALLON, B. S., MCKAY, R. D. & ROBEY, P. G. 2014. Human pluripotent stem cell culture: considerations for maintenance, expansion, and therapeutics. *Cell Stem Cell,* 14**,** 13-26.

CHERRY, A. B. & DALEY, G. Q. 2012. Reprogramming cellular identity for regenerative medicine. *Cell,* 148**,** 1110-22.

CHOI, W., PORTEN, S., KIM, S., WILLIS, D., PLIMACK, E. R., HOFFMAN-CENSITS, J., ROTH, B., CHENG, T., TRAN, M., LEE, I. L., MELQUIST, J., BONDARUK, J., MAJEWSKI, T., ZHANG, S., PRETZSCH, S., BAGGERLY, K., SIEFKER-RADTKE, A., CZERNIAK, B., DINNEY, C. P. & MCCONKEY, D. J. 2014. Identification of distinct basal and luminal subtypes of muscle-invasive bladder cancer with different sensitivities to frontline chemotherapy. *Cancer Cell,* 25**,** 152-65.

CIANCANELLI, M. J., HUANG, S. X., LUTHRA, P., GARNER, H., ITAN, Y., VOLPI, S., LAFAILLE, F. G., TROUILLET, C., SCHMOLKE, M., ALBRECHT, R. A., ISRAELSSON, E., LIM, H. K., CASADIO, M., HERMESH, T., LORENZO, L., LEUNG, L. W., PEDERGNANA, V., BOISSON, B., OKADA, S., PICARD, C., RINGUIER, B., TROUSSIER, F., CHAUSSABEL, D., ABEL, L., PELLIER, I., NOTARANGELO, L. D.,

GARCIA-SASTRE, A., BASLER, C. F., GEISSMANN, F., ZHANG, S. Y., SNOECK, H. W. & CASANOVA, J. L. 2015. Infectious disease. Life-threatening influenza and impaired interferon amplification in human IRF7 deficiency. *Science,* 348**,** 448-53.

CLEVERS, H. 2016. Modeling Development and Disease with Organoids. *Cell,* 165**,** 1586-1597.

COSENTINO, M., PALOU, J., GAYA, J. M., BREDA, A., RODRIGUEZ-FABA, O. & VILLAVICENCIO-MAVRICH, H. 2013. Upper urinary tract urothelial cell carcinoma: location as a predictive factor for concomitant bladder carcinoma. *World J Urol,* 31**,** 141-5.

CUTRESS, M. L., STEWART, G. D., WELLS-COLE, S., PHIPPS, S., THOMAS, B. G. & TOLLEY, D. A. 2012. Long-term endoscopic management of upper tract urothelial carcinoma: 20-year single-centre experience. *BJU Int,* 110**,** 1608-17.

DAMRAUER, J. S., HOADLEY, K. A., CHISM, D. D., FAN, C., TIGANELLI, C. J., WOBKER, S. E., YEH, J. J., MILOWSKY, M. I., IYER, G., PARKER, J. S. & KIM, W. Y. 2014. Intrinsic subtypes of high-grade bladder cancer reflect the hallmarks of breast cancer biology. *Proc Natl Acad Sci U S A,* 111**,** 3110-5.

DASARI, S. & TCHOUNWOU, P. B. 2014. Cisplatin in cancer therapy: molecular mechanisms of action. *Eur J Pharmacol,* 740**,** 364-78.

DEKKERS, J. F., WIEGERINCK, C. L., DE JONGE, H. R., BRONSVELD, I., JANSSENS, H. M., DE WINTER-DE GROOT, K. M., BRANDSMA, A. M., DE JONG, N. W., BIJVELDS, M. J., SCHOLTE, B. J., NIEUWENHUIS, E. E., VAN DEN BRINK, S., CLEVERS, H., VAN DER ENT, C. K., MIDDENDORP, S. & BEEKMAN, J. M. 2013. A functional CFTR assay using primary cystic fibrosis intestinal organoids. *Nat Med,* 19**,** 939-45.

DYE, B. R., HILL, D. R., FERGUSON, M. A., TSAI, Y. H., NAGY, M. S., DYAL, R., WELLS, J. M., MAYHEW, C. N., NATTIV, R., KLEIN, O. D., WHITE, E. S., DEUTSCH, G. H. & SPENCE, J. R. 2015. In vitro generation of human pluripotent stem cell derived lung organoids. *Elife,* 4.

EARL, J., RICO, D., CARRILLO-DE-SANTA-PAU, E., RODRIGUEZ-SANTIAGO, B., MENDEZ-PERTUZ, M., AUER, H., GOMEZ, G., GROSSMAN, H. B., PISANO, D. G., SCHULZ, W. A., PEREZ-JURADO, L. A., CARRATO, A., THEODORESCU, D., CHANOCK, S., VALENCIA, A. & REAL, F. X. 2015. The UBC-40 Urothelial Bladder Cancer cell line index: a genomic resource for functional studies. *BMC Genomics,* 16**,** 403.

EAU GUIDELINES. Edn. presented at the EAU Annual Congress Milan 2021. ISBN 978-94-92671-13-4.https://uroweb.org/guideline/non-muscle-invasive-bladder-cancer/#7

FREEDMAN, L. P., COCKBURN, I. M. & SIMCOE, T. S. 2015. The Economics of Reproducibility in Preclinical Research. *PLoS Biol,* 13**,** e1002165.

Genomics of Drug Sensitivity in Cancer. Retrieved November 10, 2020, From https://www.cancerrxgene.org/celllines

GOODSPEED, A., HEISER, L. M., GRAY, J. W. & COSTELLO, J. C. 2016. Tumor-Derived Cell Lines as Molecular Models of Cancer Pharmacogenomics. *Mol Cancer Res,* 14**,** 3-13.

GRIVAS, P. D., DAY, M. & HUSSAIN, M. 2011. Urothelial carcinomas: a focus on human epidermal receptors signaling. *Am J Transl Res,* 3**,** 362-73.

GUDJONSSON, T., VILLADSEN, R., NIELSEN, H. L., RONNOV-JESSEN, L., BISSELL, M. J. & PETERSEN, O. W. 2002. Isolation, immortalization, and characterization of a human breast epithelial cell line with stem cell properties. *Genes Dev,* 16**,** 693-706.

HANAHAN, D. & WEINBERG, R. A. 2000. The hallmarks of cancer. *Cell,* 100**,** 57-70.

HANAHAN, D. & WEINBERG, R. A. 2011. Hallmarks of cancer: the next generation. *Cell,* 144**,** 646-74.

HOLOHAN, C., VAN SCHAEYBROECK, S., LONGLEY, D. B. & JOHNSTON, P. G. 2013. Cancer drug resistance: an evolving paradigm. *Nat Rev Cancer,* 13**,** 714-26.

HOSOGOE, S., HATAKEYAMA, S., KUSAKA, A., HAMANO, I., IWAMURA, H., FUJITA, N., YAMAMOTO, H., TOBISAWA, Y., YONEYAMA, T., YONEYAMA, T., HASHIMOTO, Y., KOIE, T. & OHYAMA, C. 2018. Platinum-based Neoadjuvant Chemotherapy Improves Oncological Outcomes in Patients with Locally Advanced Upper Tract Urothelial Carcinoma. *Eur Urol Focus,* 4**,** 946-953.

HUCH, M. & KOO, B. K. 2015. Modeling mouse and human development using organoid cultures. *Development,* 142**,** 3113-25.

KAMAT, A. M., HAHN, N. M., EFSTATHIOU, J. A., LERNER, S. P., MALMSTROM, P. U., CHOI, W., GUO, C. C., LOTAN, Y. & KASSOUF, W. 2016. Bladder cancer. *Lancet,* 388**,** 2796-2810.

KERR, J. F., WYLLIE, A. H. & CURRIE, A. R. 1972. Apoptosis: a basic biological phenomenon with wide-ranging implications in tissue kinetics. *Br J Cancer,* 26**,** 239-57.

KESSLER, M., HOFFMANN, K., BRINKMANN, V., THIECK, O., JACKISCH, S., TOELLE, B., BERGER, H., MOLLENKOPF, H. J., MANGLER, M., SEHOULI, J., FOTOPOULOU, C. & MEYER, T. F. 2015. The Notch and Wnt pathways regulate stemness and differentiation in human fallopian tube organoids. *Nat Commun,* 6**,** 8989.

KURMANN, A. A., SERRA, M., HAWKINS, F., RANKIN, S. A., MORI, M., ASTAPOVA, I., ULLAS, S., LIN, S., BILODEAU, M., ROSSANT, J., JEAN, J. C., IKONOMOU, L., DETERDING, R. R., SHANNON, J. M., ZORN, A. M., HOLLENBERG, A. N. & KOTTON, D. N. 2015. Regeneration of Thyroid Function by Transplantation of Differentiated Pluripotent Stem Cells. *Cell Stem Cell,* 17**,** 527-42.

LANCASTER, M. A. & HUCH, M. 2019. Disease modelling in human organoids. *Dis Model Mech,* 12.

LANCASTER, M. A., RENNER, M., MARTIN, C. A., WENZEL, D., BICKNELL, L. S., HURLES, M. E., HOMFRAY, T., PENNINGER, J. M., JACKSON, A. P. & KNOBLICH, J. A. 2013. Cerebral organoids model human brain development and microcephaly. *Nature,* 501**,** 373-9.

LEE, S. H., HU, W., MATULAY, J. T., SILVA, M. V., OWCZAREK, T. B., KIM, K., CHUA, C. W., BARLOW, L. J., KANDOTH, C., WILLIAMS, A. B., BERGREN, S. K., PIETZAK, E. J., ANDERSON, C. B., BENSON, M. C., COLEMAN, J. A., TAYLOR, B. S., ABATE-SHEN, C., MCKIERNAN, J. M., AL-AHMADIE, H., SOLIT, D. B. & SHEN, M. M. 2018. Tumor Evolution and Drug Response in Patient-Derived Organoid Models of Bladder Cancer. *Cell,* 173**,** 515-528 e17.

LERNER, S. P., BAJORIN, D. F., DINNEY, C. P., EFSTATHIOU, J. A., GROSHEN, S., HAHN, N. M., HANSEL, D., KWIATKOWSKI, D., O'DONNELL, M., ROSENBERG, J., SVATEK, R., ABRAMS, J. S., AL-AHMADIE, H., APOLO, A. B., BELLMUNT, J., CALLAHAN, M., CHA, E. K., DRAKE, C., JAROW, J., KAMAT, A., KIM, W., KNOWLES, M., MANN, B., MARCHIONNI, L., MCCONKEY, D., MCSHANE, L., RAMIREZ, N., SHARABI, A., SHARPE, A. H., SOLIT, D., TANGEN, C. M., AMIRI, A. T., VAN ALLEN, E., WEST, P. J., WITJES, J. A. & QUALE, D. Z. 2016. Summary and Recommendations from the National Cancer Institute's Clinical Trials Planning Meeting on Novel Therapeutics for Non-Muscle Invasive Bladder Cancer. *Bladder Cancer,* 2**,** 165-202.

LINNEMANN, J. R., MIURA, H., MEIXNER, L. K., IRMLER, M., KLOOS, U. J., HIRSCHI, B., BARTSCH, H. S., SASS, S., BECKERS, J., THEIS, F. J., GABKA, C., SOTLAR, K. & SCHEEL, C. H. 2015. Quantification of regenerative potential in primary human mammary epithelial cells. *Development,* 142**,** 3239-51.

LUGHEZZANI, G., BURGER, M., MARGULIS, V., MATIN, S. F., NOVARA, G., ROUPRET, M., SHARIAT, S. F., WOOD, C. G. & ZIGEUNER, R. 2012. Prognostic factors in upper urinary tract urothelial carcinomas: a comprehensive review of the current literature. *Eur Urol,* 62**,** 100-14.

MALMSTROM, P. U., SYLVESTER, R. J., CRAWFORD, D. E., FRIEDRICH, M., KREGE, S., RINTALA, E., SOLSONA, E., DI STASI, S. M. & WITJES, J. A. 2009. An individual patient data meta-analysis of the long-term outcome of randomised studies comparing intravesical mitomycin C versus bacillus Calmette-Guerin for non-muscle-invasive bladder cancer. *Eur Urol,* 56**,** 247-56.

MARGULIS, V., SHARIAT, S. F., MATIN, S. F., KAMAT, A. M., ZIGEUNER, R., KIKUCHI, E., LOTAN, Y., WEIZER, A., RAMAN, J. D., WOOD, C. G. & UPPER TRACT UROTHELIAL CARCINOMA COLLABORATIONTHE UPPER TRACT UROTHELIAL CARCINOMA, C. 2009. Outcomes of radical nephroureterectomy: a series from the Upper Tract Urothelial Carcinoma Collaboration. *Cancer,* 115**,** 1224-33.

MATULEWICZ, R. S. & STEINBERG, G. D. 2020. Non-muscle-invasive Bladder Cancer: Overview and Contemporary Treatment Landscape of Neoadjuvant Chemoablative Therapies. *Rev Urol,* 22**,** 43-51.

MCCRACKEN, K. W., CATA, E. M., CRAWFORD, C. M., SINAGOGA, K. L., SCHUMACHER, M., ROCKICH, B. E., TSAI, Y. H., MAYHEW, C. N., SPENCE, J. R., ZAVROS, Y. & WELLS, J. M. 2014. Modelling human development and disease in pluripotent stem-cell-derived gastric organoids. *Nature,* 516**,** 400-4.

MOSCHINI, M., XYLINAS, E., ZAMBONI, S., MATTEI, A., NIEGISCH, G., YU, E. Y., BAMIAS, A., AGARWAL, N., SRIDHAR, S. S., STERNBERG, C. N., VAISHAMPAYAN, U. N., ROSENBERG, J. E., BELLMUNT, J., GALSKY, M. D., MONTORSI, F., NECCHI, A. & INVESTIGATORS, R. 2020. Efficacy of Surgery in the Primary Tumor Site for Metastatic Urothelial Cancer: Analysis of an International, Multicenter, Multidisciplinary Database. *Eur Urol Oncol,* 3**,** 94-101.

MULLENDERS, J., DE JONGH, E., BROUSALI, A., ROOSEN, M., BLOM, J. P. A., BEGTHEL, H., KORVING, J., JONGES, T., KRANENBURG, O., MEIJER, R. & CLEVERS, H. C. 2019. Mouse and human urothelial cancer organoids: A tool for bladder cancer research. *Proc Natl Acad Sci U S A,* 116**,** 4567-4574.

NAZZANI, S., PREISSER, F., MAZZONE, E., MARCHIONI, M., BANDINI, M., TIAN, Z., MISTRETTA, F. A., SHARIAT, S. F., SOULIERES, D., SAAD, F., MONTANARI, E., LUZZAGO, S., BRIGANTI, A., CARMIGNANI, L. & KARAKIEWICZ, P. I. 2019. Survival Effect of Nephroureterectomy in Metastatic Upper Urinary Tract Urothelial Carcinoma. *Clin Genitourin Cancer,* 17**,** e602-e611.

OU, Y. C., HU, C. Y., CHENG, H. L. & YANG, W. H. 2018. Long-term outcomes of total ureterectomy with ileal-ureteral substitution treatment for ureteral cancer: a single-center experience. *BMC Urol,* 18**,** 73.

PARFITT, D. A., LANE, A., RAMSDEN, C. M., CARR, A. F., MUNRO, P. M., JOVANOVIC, K., SCHWARZ, N., KANUGA, N., MUTHIAH, M. N., HULL, S., GALLO, J. M., DA CRUZ, L., MOORE, A. T., HARDCASTLE, A. J., COFFEY, P. J. & CHEETHAM, M. E. 2016. Identification and Correction of Mechanisms Underlying Inherited Blindness in Human iPSC-Derived Optic Cups. *Cell Stem Cell,* 18**,** 769-781.

PAULI, C., HOPKINS, B. D., PRANDI, D., SHAW, R., FEDRIZZI, T., SBONER, A., SAILER, V., AUGELLO, M., PUCA, L., ROSATI, R., MCNARY, T. J., CHURAKOVA, Y., CHEUNG, C., TRISCOTT, J., PISAPIA, D., RAO, R., MOSQUERA, J. M., ROBINSON, B., FALTAS, B. M., EMERLING, B. E., GADI, V. K., BERNARD, B., ELEMENTO, O., BELTRAN, H., DEMICHELIS, F., KEMP, C. J., GRANDORI, C., CANTLEY, L. C. & RUBIN, M. A. 2017. Personalized In Vitro and In Vivo Cancer Models to Guide Precision Medicine. *Cancer Discov,* 7**,** 462-477.

PEROU, C. M., SORLIE, T., EISEN, M. B., VAN DE RIJN, M., JEFFREY, S. S., REES, C. A., POLLACK, J. R., ROSS, D. T., JOHNSEN, H., AKSLEN, L. A., FLUGE, O., PERGAMENSCHIKOV, A., WILLIAMS, C., ZHU, S. X., LONNING, P. E., BORRESEN-DALE, A. L., BROWN, P. O. & BOTSTEIN, D. 2000. Molecular portraits of human breast tumours. *Nature,* 406**,** 747-52.

PORTEN, S., SIEFKER-RADTKE, A. O., XIAO, L., MARGULIS, V., KAMAT, A. M., WOOD, C. G., JONASCH, E., DINNEY, C. P. & MATIN, S. F. 2014. Neoadjuvant chemotherapy improves survival of patients with upper tract urothelial carcinoma. *Cancer,* 120**,** 1794-9.

PRASAD, S. M., DECASTRO, G. J., STEINBERG, G. D. & MEDSCAPE 2011. Urothelial carcinoma of the bladder: definition, treatment and future efforts. *Nat Rev Urol,* 8**,** 631-42.

PRINZ, F., SCHLANGE, T. & ASADULLAH, K. 2011. Believe it or not: how much can we rely on published data on potential drug targets? *Nat Rev Drug Discov,* 10**,** 712.

RASMUSSEN, R., MORRISON, T., HERRMANN, M. & WITTWER, C. 1998. Quantitative PCR by contiuous fluorescence monitoring of a double strand DNA specific binding dye. *Biochimica,* 2: 8 – 11.

RESNICK, M. J., BASSETT, J. C. & CLARK, P. E. 2013. Management of superficial and muscle-invasive urothelial cancers of the bladder. *Curr Opin Oncol,* 25**,** 281-8.

ROUPRET, M., BABJUK, M., BURGER, M., CAPOUN, O., COHEN, D., COMPERAT, E. M., COWAN, N. C., DOMINGUEZ-ESCRIG, J. L., GONTERO, P., HUGH MOSTAFID, A., PALOU, J., PEYRONNET, B., SEISEN, T., SOUKUP, V., SYLVESTER, R. J., RHIJN, B., ZIGEUNER, R. & SHARIAT, S. F. 2021. European Association of Urology Guidelines on Upper Urinary Tract Urothelial Carcinoma: 2020 Update. *Eur Urol,* 79**,** 62-79.

ROUPRET, M., COLIN, P. & YATES, D. R. 2014. A new proposal to risk stratify urothelial carcinomas of the upper urinary tract (UTUCs) in a predefinitive treatment setting: low-risk versus high-risk UTUCs. *Eur Urol,* 66**,** 181-3.

ROUPRêT, M., HUPERTAN, V., SEISEN, T., COLIN, P., XYLINAS, E., YATES, D. R., FAJKOVIC, H., LOTAN, Y., RAMAN, J. D., ZIGEUNER, R., REMZI, M., BOLENZ, C., NOVARA, G., KASSOUF, W., OUZZANE, A., ROZET, F., CUSSENOT, O., MARTINEZ-SALAMANCA, J. I., FRITSCHE, H. M., WALTON, T. J., WOOD, C. G., BENSALAH, K., KARAKIEWICZ, P. I., MONTORSI, F., MARGULIS, V. & SHARIAT, S. F. 2013. Prediction of cancer specific survival after radical nephroureterectomy for upper tract urothelial carcinoma: development of an optimized postoperative nomogram using decision curve analysis. *J Urol,* 189**,** 1662-9.

SATO, T., STANGE, D. E., FERRANTE, M., VRIES, R. G., VAN ES, J. H., VAN DEN BRINK, S., VAN HOUDT, W. J., PRONK, A., VAN GORP, J., SIERSEMA, P. D. & CLEVERS, H. 2011. Long-term expansion of epithelial

organoids from human colon, adenoma, adenocarcinoma, and Barrett's epithelium. *Gastroenterology,* 141**,** 1762-72.

SATO, T., VRIES, R. G., SNIPPERT, H. J., VAN DE WETERING, M., BARKER, N., STANGE, D. E., VAN ES, J. H., ABO, A., KUJALA, P., PETERS, P. J. & CLEVERS, H. 2009. Single Lgr5 stem cells build crypt-villus structures in vitro without a mesenchymal niche. *Nature,* 459**,** 262-5.

SEISEN, T., PEYRONNET, B., DOMINGUEZ-ESCRIG, J. L., BRUINS, H. M., YUAN, C. Y., BABJUK, M., BOHLE, A., BURGER, M., COMPERAT, E. M., COWAN, N. C., KAASINEN, E., PALOU, J., VAN RHIJN, B. W., SYLVESTER, R. J., ZIGEUNER, R., SHARIAT, S. F. & ROUPRET, M. 2016. Oncologic Outcomes of Kidney-sparing Surgery Versus Radical Nephroureterectomy for Upper Tract Urothelial Carcinoma: A Systematic Review by the EAU Non-muscle Invasive Bladder Cancer Guidelines Panel. *Eur Urol,* 70**,** 1052-1068.

SHARMA, S. V., HABER, D. A. & SETTLEMAN, J. 2010. Cell line-based platforms to evaluate the therapeutic efficacy of candidate anticancer agents. *Nat Rev Cancer,* 10**,** 241-53.

SHELLEY, M. D., KYNASTON, H., COURT, J., WILT, T. J., COLES, B., BURGON, K. & MASON, M. D. 2001. A systematic review of intravesical bacillus Calmette-Guerin plus transurethral resection vs transurethral resection alone in Ta and T1 bladder cancer. *BJU Int,* 88**,** 209-16.

SIEGEL, R. L., MILLER, K. D., FUCHS, H. E. & JEMAL, A. 2021. Cancer Statistics, 2021. *CA Cancer J Clin,* 71**,** 7-33.

SIEGEL, R. L., MILLER, K. D. & JEMAL, A. 2019. Cancer statistics, 2019. *CA Cancer J Clin,* 69**,** 7-34.

SMITH, E. & COCHRANE, W. J. 1946. CYSTIC ORGANOID TERATOMA: (Report of a Case). *Can Med Assoc J,* 55**,** 151-2.

TAKEBE, T., SEKINE, K., ENOMURA, M., KOIKE, H., KIMURA, M., OGAERI, T., ZHANG, R. R., UENO, Y., ZHENG, Y. W., KOIKE, N., AOYAMA, S., ADACHI, Y. & TANIGUCHI, H. 2013. Vascularized and functional human liver from an iPSC-derived organ bud transplant. *Nature,* 499**,** 481-4.

TSUTSUMI, Y. 2021. Pitfalls and Caveats in Applying Chromogenic Immunostaining to Histopathological Diagnosis. *Cells,* 10.

TURCO, M. Y., GARDNER, L., HUGHES, J., CINDROVA-DAVIES, T., GOMEZ, M. J., FARRELL, L., HOLLINSHEAD, M., MARSH, S. G. E., BROSENS, J. J., CRITCHLEY, H. O., SIMONS, B. D., HEMBERGER, M., KOO, B. K., MOFFETT, A. & BURTON, G. J. 2017. Long-term, hormone-responsive organoid cultures of human endometrium in a chemically defined medium. *Nat Cell Biol,* 19**,** 568-577.

VAN RHIJN, B. W., ZUIVERLOON, T. C., VIS, A. N., RADVANYI, F., VAN LEENDERS, G. J., OOMS, B. C., KIRKELS, W. J., LOCKWOOD, G. A., BOEVE, E. R., JOBSIS, A. C., ZWARTHOFF, E. C. & VAN DER KWAST, T.

H. 2010. Molecular grade (FGFR3/MIB-1) and EORTC risk scores are predictive in primary non-muscle-invasive bladder cancer. *Eur Urol,* 58**,** 433-41.

VEMANA, G., KIM, E. H., BHAYANI, S. B., VETTER, J. M. & STROPE, S. A. 2016. Survival Comparison Between Endoscopic and Surgical Management for Patients With Upper Tract Urothelial Cancer: A Matched Propensity Score Analysis Using Surveillance, Epidemiology and End Results-Medicare Data. *Urology,* 95**,** 115-20.

VILLALOBOS-ORTIZ, M., RYAN, J., MASHAKA, T. N., OPFERMAN, J. T. & LETAI, A. 2020. BH3 profiling discriminates on-target small molecule BH3 mimetics from putative mimetics. *Cell Death Differ,* 27**,** 999-1007.

ZHANG, Y. & ZHENG, J. 2020. Functions of Immune Checkpoint Molecules Beyond Immune Evasion. *Adv Exp Med Biol,* 1248**,** 201-226.

7 Declaration

The experiments for this thesis were carried out in the laboratories of the Department of Urology at the University of Tuebingen Hospital (UKT) at the Center for Medical Research (ZMF) under the supervision of Prof. Dr. rer. nat. Wilhelm K. Aicher. The study was supported by a stipend provided by the Second Affiliated Hospital of Guilin Medical University and was designed and supported by Dr. med. Niklas Harland. The experiments were carried out independently by myself (after training by laboratory members). The training included the generation of the following organoids which therefore will also be part of the thesis of Leander Schwaibold: BCO#41, BCO#44, RTO#4, and BCO#56. However, all cytotox assays including their evaluation were performed by myself. Surgical samples were provided by the Dept. of Urology. I assure you that I have written the manuscript myself and that I have not used any other sources than those given by me.

Tübingen, March 10th, 2022

Yi Wei

8 Acknowledgement

I would like to take this opportunity to thank my supervisor Prof. Arnulf Stenzl for providing the lab space and offering the chance to study in Tubingen in Germany as well as for his excellent support during my whole doctoral period.

My special thanks must be for Prof. Wilhelm K. Aicher. I learned a lot from him and will always remember a “eyes to eyes” moment at a Tuesday morning and cute look that is always energetic. Without his teaching, guidance and help, I think I will never finish my work in time.

Moreover, I would like to thank my special supervisor Dr. Niklas Harland. The man who first time take me to operation room, to help me complete registration, and to teach me how to make presentation in the conference.

I also thank my colleagues Christine, Tanja, Conny, Jasmin, Nizar, Paul, Johannes, Ingrid and special Lenny for all the assistance of my work and life. I regret that I can’t speak German and missed a lot of time to chat with everyone.

I also would like to thank my previous supervisor Prof. Zhang and Prof. Ge for their concern since the master’s study. Furthermore, I would like to thank my friend Ruizhi, Sheng, Xioaning, Nan, Hong, Lingjun, Ge, Yanjun and Hongrui for sharing a great time during my Germany life.

Lastly, a great special thanks to my family, especially my mother. Without their support and love, I could not persist such a long time to complete my studies.

Thanks, the city, university, UKT, ZMF and everything of Tuebingen. This unique journey must be indelible in my life.

Tübingen, 10.03.2022

9 Abstracts / manuscripts

9.1 Abstracts

1. **Yi Wei**, Leander Schwaibold, Tilman Todenhöfer, Arnulf Stenzl. Wilhelm K. Aicher, Niklas Harland. (2021). Methodology of drug testing using patient derived organoids of upper tract urothelial carcinoma. *European Urology*, supplement 1,abstract only volume 79, S639.

2. **Yi Wei**, T Todenhöfer, L Schwaibold, A Stenzl, W.K Aicher, N Harland. (2021). Drug testing using patient derived organoids from upper tract urothelial carcinoma and bladder cancer. *Der Urology*, suppl 1, S85.

3. **Yi Wei**, B. Amend, A. Stenzl, W. K. Aicher, N. Harland. (2022). Cytotoxicity caused by cisplatin, venetoclax, and S63845 to urothelial carcinoma cells expanded in 3D organoids differs clearly from cytotoxicity to autologous 2D adherent cells. *Journal of Urology*. Volume 207, Issue Supplement 5.

9.2 manuscripts

1. **Yi Wei**, Bastian Amend, Tilman Todenhöfer, Nizar Lipke, Wilhelm K. Aicher, Falko Fend, Arnulf Stenzl, and Niklas Harland. (2022). Urinary Tract Tumor Organoids Reveal Eminent Differences in Drug Sensitivities When Compared to 2-Dimensional Culture Systems. *Int J Mol Sci*, 23.

2. **Yi Wei**, Arnulf Stenzl., et al. Screening target-specific anti-tumor drugs in bladder cancer cells in 2D versus 3D cell cultures. (Manuscript preparation)